

**Optimized synthesis of π -extended squaraine dyes relevant to organic electronics by
direct (hetero)arylation and Sonogashira coupling reactions**

Abby-Jo Payne and Gregory C. Welch*
Department of Chemistry, University of Calgary
2500 University Drive NW Calgary, AB, Canada T2N 1N4

* Corresponding Author
Email: gregory.welch@ucalgary.ca
Phone Number: 1-403-210-7603

SUPPORTING INFORMATION

Table of Contents

Materials and Methods	S3
Experimental	S5
Solution NMR Spectra	S18
Mass Spectrometry (MALDI-TOF)	S39
Emission Spectra	S43
Thermal Gravimetric Analysis (TGA)	S43
Density Functional Theory	S44
XRD	S49
Tabulated CV and Optical Data for 9b and 9Th	S50
References	S51

Materials and Methods

Materials: Pivalic acid (PivOH) was purchased from TCI America and 6-bromo-2-oxindole was acquired from Ontario Chemicals Inc. Siliacat® DPP-Pd was received from SiliCycle and all other catalysts were purchased from Strem Chemicals. 4,5-difluoro-1,2-phenylenediamine was obtained from ACROS Organics. The remaining reagents were purchased from Sigma-Aldrich. All solvents and materials purchased were used without further purification. Purification by flash column chromatography was performed using a Biotage® Isolera flash system.

Microwave-Assisted Synthesis: All microwave reactions were carried out using a Biotage® Initiator+ microwave reactor. The operational power range of the instrument is 0–400 W, using a 2.45 GHz magnetron. Pressurized air is used to cool each reaction after microwave heating.

Nuclear Magnetic Resonance (NMR): ¹H and ¹³C{¹H} NMR spectroscopy spectra were recorded on a Bruker Avance-500 MHz spectrometer at 300 K. Chemical shifts are reported in parts per million (ppm). Multiplicities are reported as: singlet (s), doublet (d), doublet of doublets (dd), triplet (t), multiplet (m), quintet (quin), overlapping (ov), and broad (br).

High-resolution Mass Spectrometry (HRMS): High-resolution MALDI mass spectrometry measurements were performed courtesy of Jian Jun (Johnson) Li in the Chemical Instrumentation Facility at the University of Calgary. A Bruker Autoflex III Smartbeam MALDI-TOF (Na:YAG laser, 355nm), setting in positive reflective mode, was used to acquire spectra. Operation settings were all typical, e.g. laser offset 62-69; laser frequency 200Hz; and number of shots 300. The target used was Bruker MTP 384 ground steel plate target. Sample solution (~ 1 µg/mL in dichloromethane) was mixed with matrix trans-2-[3-(4-tert-Butylphenyl)-2-methyl-2-propenyldene]malononitrile (DCTB) solution (~ 5mg/mL in methanol). Pipetted 1µl solution above to target spot and dried in the fume hood.

Cyclic Voltammetry (CV): All electrochemical measurements were performed using a Model 1200B Series Handheld Potentiostat by CH Instruments Inc. equipped with Ag wire, Pt wire and glassy carbon electrode, as the pseudo reference, counter electrode and working electrode, respectively. Glassy carbon electrodes were polished with alumina. The cyclic voltammetry experiments were performed in anhydrous dichloromethane solution with ~0.1 M tetrabutylammonium hexafluorophosphate (TBAPF₆) as the supporting electrolyte at scan rate 100 mV/s. All electrochemical solutions were purged with dry N₂ for 5 minutes to deoxygenate the system. Solution CV measurements were carried out with a small molecule concentration of ~0.5 mg/mL in dichloromethane. Ferrocene was used as an internal standard. The IPs and EAs were estimated using the onsets of oxidation and reduction referenced to the Fc/Fc⁺ redox couple and a conversion factor of 4.8.

UV-Visible Spectroscopy (UV-Vis): All absorption measurements were recorded using Agilent Technologies Cary 60 UV-Vis spectrometer at room temperature. All solution UV-

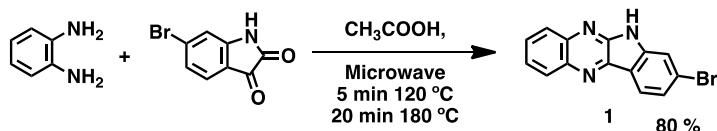
Vis experiments were run in CHCl_3 using 10 mm quartz cuvettes. Neat films were prepared by spin-coating ~ 0.2 mL from a 1 % wt/v solution (CHCl_3) onto clean UV-ozoned glass substrates coated with PEDOT:PSS. Spin-coating details: 2500 RPM 10,000 RPM/s² for 30 seconds. PEDOT:PSS was used to coat the glass to ensure uniform film formation. Same optical absorption results were obtained without the use of PEDOT:PSS, but films were not as uniform. Films were thermally annealed by direct mounting on a VWR hotplate. Films solvent vapour annealed by placing in a glass jar with appropriate solvent and sealed. Films were thermally annealing from 100°C to 200°C with 10°C intervals. Annealing temperatures noted in the paper are where major changes were observed. Films were solvent vapour annealed for up to 20 minutes, checking the profiles at 5 minute intervals. Times noted in the paper are where major changes were observed, or in the case of **10** no changes were observed at all.

Photoluminescence (PL): All emission measurements were recorded using Agilent Technologies Cary Eclipse Fluorescence spectrophotometer at room temperature. All solution PL experiments were run in CHCl_3 using 10 mm quartz cuvettes.

X-ray Diffraction (XRD): Thin film XRD analysis of **13** (1% w/v CHCl_3 2500 RPM, 10,000 RPM/s², 30 s spun cast on quartz substrates) were performed on a PROTO AXRD benchtop powder diffractometer with Cu K α radiation operating at a power level of 30 kV and 20 mA. Samples were scanned in plane (θ -2 θ scans) from 4°-8° 2 θ using a $\Delta 2\theta^\circ$ of 0.01963, a dwell time of 40 s, and a 0.5 mm divergence slit.

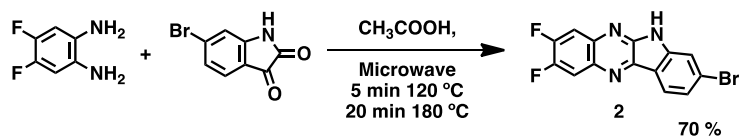
Experimental:

Synthesis of 8-bromo-6H-indolo[2,3-b]quinoxaline (1).



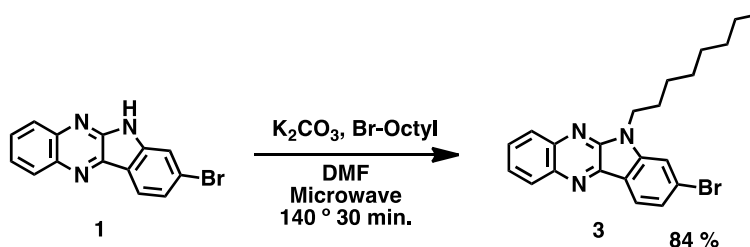
A solution of 6-bromoisatin (1000 mg, 4.42 mmol) and *o*-phenylenediamine (480 mg, 4.44 mmol) in glacial acetic acid (24 mL) was sealed in a pressure tube with a Teflon® cap and heated for five minutes at 120 °C followed by 20 minutes at 180 °C. The reaction mixture was stirred in H₂O (400 mL) for two hours. The resulting yellow solid was collected via vacuum filtration and washed with copious amounts of water followed by recrystallization from EtOH (50 mL). The solid was dried *in vacuo* to yield **1** (1050 mg, 3.52 mmol, 80 % yield) as a light yellow powder. ¹H NMR Corresponds to literature.¹

Synthesis of 8-bromo-2,3-difluoro-6H-indolo[2,3-b]quinoxaline (2).



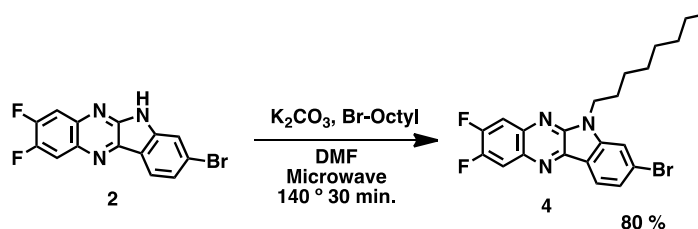
Compound **2** was synthesized following the same scale and conditions for **1** substituting *o*-phenylene diamine for 4,5-difluoro-1,2-phenylenediamine and was isolated as green solid (70 % yield). ¹H NMR (500 MHz, DMSO-d₆, ppm): δ 12.31 (s, br, 1H), 8.27-8.22 (m, ov, 2H), 8.09 (dd, ¹J = 8.4 Hz, ²J = 3.3 Hz, 1H), 7.74 (d, J = 1.6 Hz, 1H), 7.52 (dd, ¹J = 6.6 Hz, ²J = 1.7 Hz, 1H) ¹⁹F NMR (500 MHz, DMSO-d₆, ppm) δ -133.846 (d, ¹J = 24.25 Hz) -137.630 (d, ¹J = 24.25 Hz) ¹³C NMR (500 MHz, CDCl₃, ppm): δ 150.53 (dd, ¹J_{C-F} = 224.12 Hz, ²J_{C-F} = 16.36 Hz), 148.55 (dd ¹J_{C-F} = 222.03 Hz, ²J_{C-F} = 16.49 Hz), 145.65, 144.42, 138.97, 137.24 (d ³J_{C-F} = 11.62 Hz), 135.24 (d ³J_{C-F} = 10.60 Hz), 124.41, 123.73, 123.66, 117.47, 114.60, 114.59 (d ²J_{C-F} = 16.99 Hz), 113.19 (d ²J_{C-F} = 17.82 Hz). Expected: 14 Found: 14.

Synthesis of 8-bromo-*N*-octyl-indolo[2,3-*b*]quinoxaline (3).



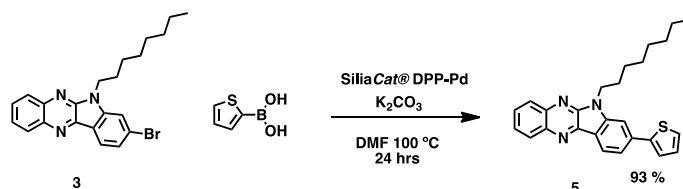
A solution of 8-bromo-indolo[2,3-*b*]quinoxaline (**1**) (400 mg, 1.34 mmol), K_2CO_3 (280 mg, 2.02 mmol), 1-octylbromide (0.3 mL, 1.34 mmol) in anhydrous DMF (5 mL) was heated to $140^\circ C$ for 30 minutes under microwave irradiation in a 10 mL pressure tube sealed under N_2 with a Teflon® cap. The reaction was cooled to room temperature and poured into a 1:1 solution of H_2O :MeOH (~100 mL) and stirred for two hours. A bright orange solid was recovered via suction filtration. The solid was washed with copious amounts of water followed by 100 mL of 2:1 H_2O :MeOH solution. The resulting solid was dried *in vacuo* to yield the alkylated product (**3**) as a yellow-orange powder (460 mg, 1.12 mmol, 84 % yield). 1H NMR Corresponds to literature.¹

Synthesis of 8-bromo-2,3-difluoro-6-octyl-6H-indolo[2,3-*b*]quinoxaline (4).



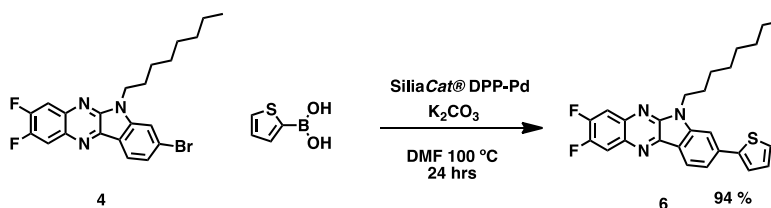
Compound **4** was prepared following the reaction procedure for **3** and was isolated as a green solid (80 % yield). 1H NMR (500 MHz, $CDCl_3$, ppm): δ 8.29 (d, $^1J=8.2$ Hz, 1H), 8.02 (dd, $^1J=8.4$ Hz, $^2J=2.5$ Hz, 1H), 7.87 (dd, $^1J=8.2$ Hz, $^2J=3.0$ Hz, 1H), 7.65 (d, $^1J=1.5$ Hz, 1H), 7.53 (dd, $^1J=1.6$ Hz, $^2J=6.7$ Hz, 1H), 4.43 (t, 2H), 1.93 (quin, 2H), 1.40 (m, 4H), 1.26 (m, 6H), 0.87 (t, 3H). ^{19}F NMR (500 MHz, $CDCl_3$, ppm) δ -133.506 (d, $^1J=22.65$ Hz) -136.372 (d, $^1J=22.95$ Hz). ^{13}C NMR (500 MHz, $CDCl_3$, ppm): δ 151.25 (dd, $^1J_{C-F}=226.49$ Hz, $^2J_{C-F}=15.89$ Hz), 149.24 (dd, $^1J_{C-F}=224.15$ Hz, $^2J_{C-F}=16.19$ Hz), 144.98, 144.26, 138.66, 137.20 (d $^3J_{C-F}=11.45$ Hz), 135.48 (d $^3J_{C-F}=10.13$ Hz), 124.87, 123.79, 123.20, 117.37, 114.18 (d $^2J_{C-F}=20.08$ Hz), 112.66 (d $^2J_{C-F}=20.08$ Hz), 112.36, 41.12, 31.21, 28.62, 28.59, 27.79, 26.41, 22.04, 13.51. Expected: 22 Found 22.

Synthesis of 6-octyl-8-(thiophen-2-yl)-6H-indolo[2,3-b]quinoxaline (5).



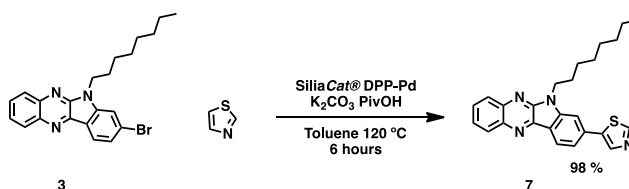
Compound **3** (555 mg, 1.35 mmol), 2-thienylboronic acid (278 mg, 2.17 mmol), SiliaCat® DPP-Pd (220 mg, 0.055 mmol Pd), and potassium carbonate (287 mg, 2.08 mmol) were added to a 20 mL pressure tube and sealed under N₂ with a Teflon® cap. Anhydrous DMF (12 mL) was syringed into the vessel and the reaction mixture was stirred and heated at 100 °C in a bead bath for 24 hours. The cooled mixture was sent through a short silica plug with DCM to remove inorganics and the heterogeneous Pd catalyst. The solvent was removed under reduced pressure and the resulting material was slurried in a minimum amount of cold hexanes and filtered yielding **5** as a fine yellow powder. (520 mg, 1.26 mmol, 93 % yield). ¹H NMR (500 MHz, CDCl₃, ppm): δ 8.47 (d, ¹J = 10 Hz, 1H), 8.29 (dd, ¹J = 9.25 Hz, ²J = 0.9 Hz, 1H), 8.14 (dd, ¹J = 9.15 Hz, ²J = 0.85 Hz, 1H), 7.75-7.78 (m, 1H) 7.66-7.71 (m, ov, 3H), 7.53 (d, ¹J = 4.25 Hz, 1H), 7.41 (d, ¹J = 5.05, 1H), 7.18 (t, 1H), 4.54 (t, 2H), 2.00 (quin, 2H), 1.39-1.47 (m, 4H), 1.22-1.31 (m, 6H), 0.86 (t, 3H). ¹³C NMR (500 MHz, CDCl₃, ppm): δ 145.59, 144.38, 143.85, 140.01, 139.13, 138.87, 136.53, 128.67, 128.08, 127.79, 127.27, 125.45, 125.42, 123.80, 122.57, 118.50, 117.99, 105.87, 40.84, 31.25, 28.69, 28.62, 27.89, 26.47, 22.06, 13.53. Expected: 26 Found: 26

Synthesis of 2,3-difluoro-6-octyl-8-(thiophen-2-yl)-6H-indolo[2,3-b]quinoxaline (6).



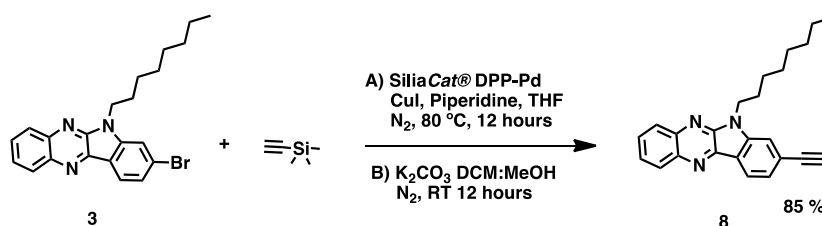
Compound **6** was prepared following the reaction procedure for **5** and was isolated a yellow/brown solid (94 % yield). ¹H NMR (500 MHz, CDCl₃, ppm): δ 8.41 (d, ¹J = 7.9 Hz, 1H), 8.01 (dd, ¹J = 8.4 Hz, ²J = 2.6 Hz, 1H), 7.86 (dd, ¹J = 8.2 Hz, ²J = 3.1 Hz, 1H) 7.65 (d, ¹J = 1.5 Hz, 1H), 7.53 (dd, ¹J = 1.6 Hz, ²J = 6.7 Hz, 1H), 4.43 (t, 2H), 1.93(quin, 2H), 1.40 (m, 4H), 1.26 (m, 6H), 0.87 (t, 3H). ¹⁹F NMR (500 MHz, DMSO-d₆, ppm) δ -133.294 (d, ¹J = 23.00 Hz) -137.063 (d, ¹J = 22.80 Hz). ¹³C NMR (500 MHz, CDCl₃, ppm): δ 151.03 (dd, ¹J_{C-F} = 235.07 Hz, ²J_{C-F} = 16.64 Hz), 149.03 (dd ¹J_{C-F} = 219.25 Hz, ²J_{C-F} = 15.72 Hz), 145.52, 144.19, 143.64, 139.13, 137.02 (d ³J_{C-F} = 10.95 Hz), 136.86, 135.42 (d ³J_{C-F} = 9.93 Hz), 127.82, 125.61, 123.92, 122.59, 118.74, 117.52, 114.09 (d ²J_{C-F} = 17.54 Hz), 112.80 (d ²J_{C-F} = 17.54 Hz), 105.90, 40.92, 31.23, 28.64, 28.59, 27.86, 26.44, 22.04, 13.50. Expected: 26 Found: 26

Synthesis of 2-(6-octyl-6H-indolo[2,3-b]quinoxalin-8-yl)thiazole (7).



A solution of **3** (695, 1.69 mmol), thiazole (322 mg, 2.78 mmol), K₂CO₃ (540 mg, 3.91 mmol), pivalic acid (65 mg, 0.637 mmol) and SiliaCat® DPP-Pd (200 mg, 0.05 mmol Pd) in 11 mL toluene was sealed in a 10 mL pressure vial under N₂ with a Teflon® cap. The reaction mixture was heated and stirred at 120 °C for 6 hours. The reaction mixture was then cooled to room temperature and sent through a short silica plug to remove the inorganics and rinsed with EtOAc to elute the product. The solvent was removed and the material was purified via column chromatography with a gradient of hexanes to ethyl acetate with product elution at 30% ethyl acetate. After solvent removal, the resulting material was slurried in 3:1 methanol:water and filtered washing with a minimal amount of cold hexanes (~5 mL) to yield **7** as a bright yellow solid (690 mg, 1.66 mmol, 98% yield). ¹H NMR (500 MHz, CDCl₃, ppm): δ 8.86 (s, 1H), 8.50 (d, ¹J=8.0 Hz, 1H), 8.30 (dd, ¹J= 1.1 Hz, ²J= 7.2 Hz, 1H), 8.28 (s, 1H), 8.15 (dd, ¹J= 1.1 Hz, ²J= 7.3 Hz, 1H), 7.18 (m, 1H), 7.70 (m, 1H), 7.63 (s, 1H), 7.61 (dd, ¹J= 1.5 Hz, ²J= 6.6 Hz, 1H), 4.53 (t, 2H), 2.00 (quin, 2H), 1.42 (m, 4H), 1.25 (m, 6H), 0.85 (t, 3H). ¹³C NMR (500 MHz, CDCl₃, ppm): δ 152.28, 145.55, 144.21, 140.17, 139.42, 139.06, 138.94, 138.79, 133.02, 128.74, 128.37, 127.33, 125.63, 122.82, 119.37, 118.90, 106.99, 40.94, 31.22, 28.66, 28.59, 27.89, 26.46, 22.03, 13.49. Expected: 25 Found: 25

Synthesis of 8-ethynyl-6-octyl-6H-indolo[2,3-b]quinoxaline (8).



A solution of **3** (310, 0.76 mmol), trimethylsilylacetylene (200 mg, 2.04 mmol), CuI (30 mg, 0.158 mmol), SiliaCat® DPP-Pd (153 mg, 0.038 mmol Pd) in 4:1 THF:piperidine (4 mL THF, 1 mL piperidine) was sealed in a 10 mL pressure vial under N₂ with a Teflon® cap. The reaction mixture was heated and stirred at 80 °C for 12 hours. The reaction mixture was then cooled to room temperature and sent through a short silica plug rinsing with hexanes (100 mL) which was discarded. Next, using 50/50 DCM/Hexanes the yellow band was eluted from the silica careful not to pull off the slower brown band. The solvent was removed and the resulting yellow oil was stirred in 2:1 DCM/MeOH (8 mL) with excess K₂CO₃ (425mg, 3.08 mmol) under N₂ at room

temperature until completion by TLC (~3-6 hours). The material was rinsed through a short silica plug with DCM. The solvent was removed and the resulting material was slurried in H₂O:MeOH (3:1) filtered to isolated **8** as a yellow solid (230 mg, 0.65, 85%)
¹H NMR (500 MHz, CDCl₃, ppm): δ 8.43 (dd, ¹J=1.0 Hz, ¹J=7.5 Hz, 1H), 8.30 (dd, ¹J=1.1 Hz, ²J=7.4 Hz, 1H), 8.15 (dd, ¹J=1.0 Hz, ²J=7.5 Hz, 1H), 7.78 (m, 1H), 7.67 (m, 1H), 7.61 (s, 1H) 7.51 (dd, ¹J=1.2 Hz, ²J=6.8 Hz, 1H), 4.48 (t, 2H), 1.95(quin, 2H), 1.40 (m, 4H), 1.26 (m, 6H), 0.87 (t, 3H). ¹³C NMR (500 MHz, CDCl₃, ppm): δ 145.48, 143.31, 140.23, 138.92, 138.74, 128.82, 128.49, 127.33, 125.62, 124.13, 123.61, 122.00, 119.21, 112.54, 83.51, 78.46, 40.98, 31.23, 28.67, 28.61, 27.86, 26.45, 22.04, 13.51. Expected: 24 Found: 24.

Synthesis of **9** and **9b**.

Both the brominated and non-brominated bis-indole squaraines, **9** and **9b** respectively, were prepared according to literature procedures. ¹H NMR spectra correspond to literature.²

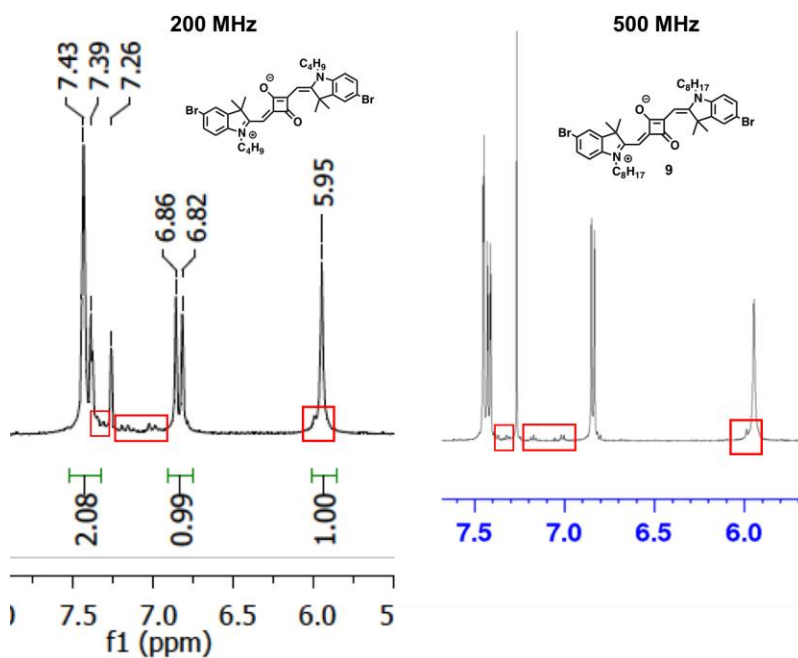


Figure S1. ¹H NMR spectrum (200 MHz) of an alkyl chain derivative (left) and ¹H NMR spectrum (500 MHz) of **9** synthesized in our lab (right), both of which contain the same trace aromatic impurities highlighted by red boxes.³

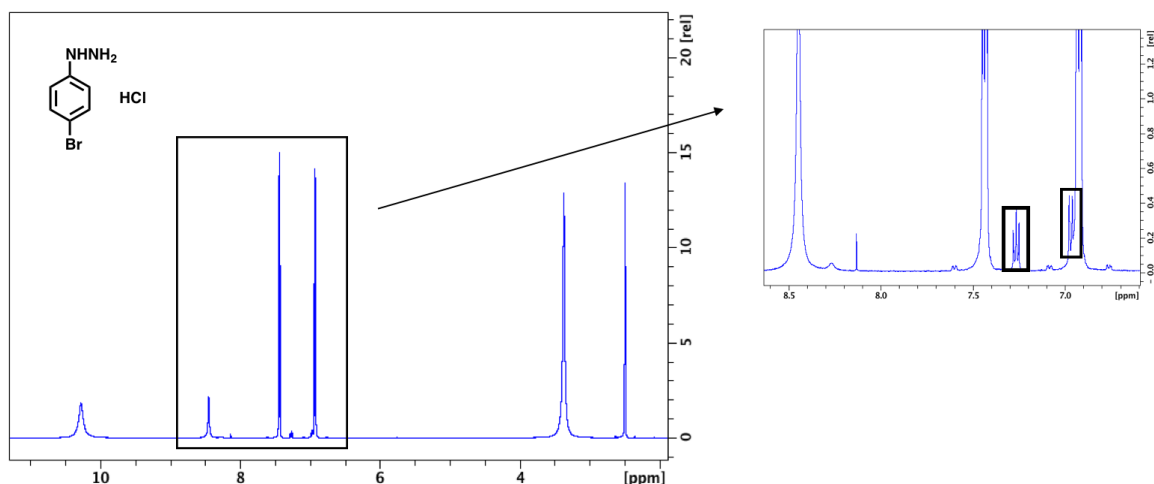
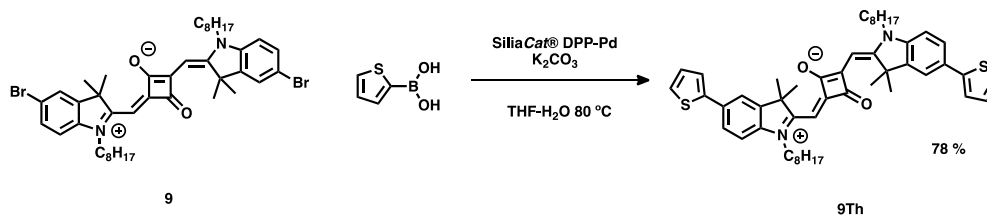


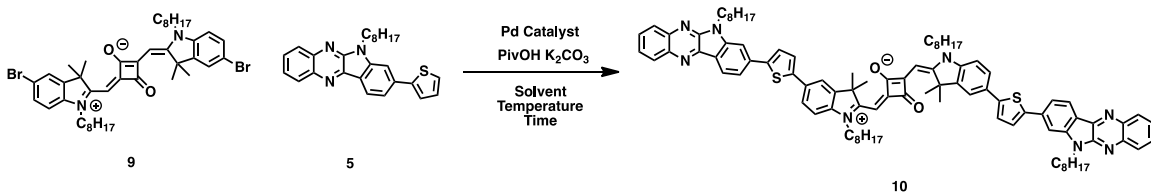
Figure S2. ^1H NMR spectrum (DMSO-D_6) of 4-bromophenylhydrazine purchased from Sigma Aldrich.

Synthesis of 9Th.



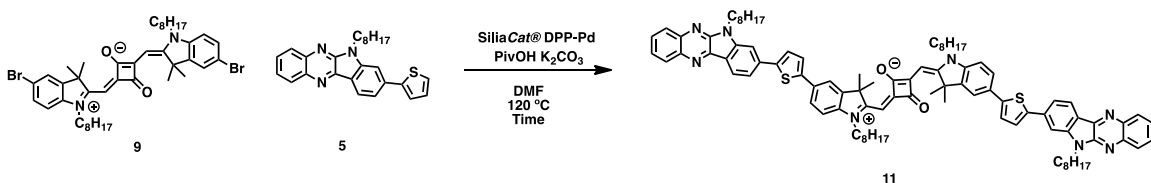
Compound **9** (105mg, 0.135 mmol), 2-thienylboronic acid (39 mg, 0.305 mmol), SiliaCat® DPP-Pd (53 mg, 0.013 mmol), and potassium carbonate (53 mg, 0.383 mmol) were added to a 10 mL pressure vial and sealed under N_2 with a Teflon® cap. Degassed THF (2 mL) and water (0.5 mL) were syringed into the vessel and the reaction mixture was stirred and heated at 80 °C in a bead bath for 24 hours. The cooled mixture was sent through a short silica plug with THF to remove inorganics and Pd catalyst. The solvent was subsequently removed under reduced pressure. The resulting shiny iridescent material was dissolved in THF (2 mL) with heat and layered with petroleum ether (8 mL). The flask was corked and placed in the fridge overnight. The resulting shiny rust coloured crystals were filtered and washed with petroleum ether (20 mL) and dried under vacuum (83 mg, 78% yield). ^1H NMR (500 MHz, CDCl_3 , ppm): δ 7.55-7.57 (m,ov, 2H), 7.31 (dd, $^1J=2.5$ Hz, $^2J=1.1$ Hz, 1H), 7.28 (dd, $^1J=12.4$ Hz, $^2J=1.1$ Hz, 1H), 7.18 (t, 1H), (6.98 (d, $^1J=8.7$ Hz, 1H), 3.99 (s, 2H), 1.84 (m, br, 6H), 1.23-1.47 (m, ov, 12H), 0.89 (t, 3H) ^{13}C NMR (500 MHz, CDCl_3 , ppm): δ 181.79, 178.90, 168.96, 143.52, 142.46, 141.40, 129.82, 127.58, 125.2, 124.03, 122.29, 119.43, 109.06, 86.49, 48.73, 43.32, 31.18, 28.78, 28.60, 26.58, 26.54, 22.05, 13.53. Expected: 50 Found: 23.

Synthesis of 10.



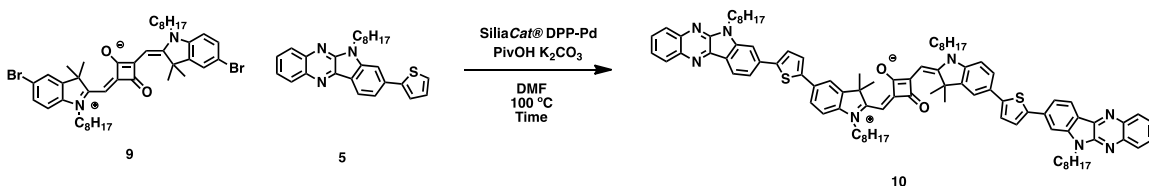
In order to optimize the direct heteroarylation reaction between **9** and **5** to form **10**, various reaction temperatures, times, catalyst systems and solvents were screened. All reactions were done on a 100 mg scale of **9** (100 mg, 0.128 mmol) with two equivalents of **5** (106 mg, 0.256 mmol), 10 mol % catalyst, 30 mol % pivalic acid (8 mg, 0.078 mmol), and two equivalents of potassium carbonate (39 mg, 0.282 mmol) in 4 mL of anhydrous degassed solvent. Reactions were heated in a Lab Armor[®] bead bath in a sealed 10 mL pressure tubes under N₂ with Teflon[®] caps. Completed reactions were cooled to room temperature, poured in 50 mL MeOH, and stirred for two hours. The resulting dark green precipitate was filtered, dissolved in DCM, and dry loaded onto silica. Column chromatography using a gradient of hexanes to THF was used with product elution at 100 % THF. The solvent was removed from the product fraction and the resulting material was slurried in MeOH and filtered. Upon drying of the material under vacuum overnight, the isolated yields and ¹H NMR (CDCl₃) spectra were recorded.

The temperature and time were first optimized using DMF as the solvent and SiliaCat[®] DPP-Pd as the catalyst.



Solvent	Catalyst	Temperature	Time	Isolated yield
DMF	SiliaCat [®] DPP-Pd	120 °C	12 hours	51 %
DMF	SiliaCat [®] DPP-Pd	120 °C	18 hours	36 %
DMF	SiliaCat [®] DPP-Pd	120 °C	24 hours	5 %

The reaction temperature was lowered to 100 °C as decomposition **9** was observed.



Solvent	Catalyst	Temperature	Time	Isolated yield
DMF	SiliaCat® DPP-Pd	100 °C	12 hours	55 %
DMF	SiliaCat® DPP-Pd	100 °C	18 hours	49 %
DMF	SiliaCat® DPP-Pd	100 °C	24 hours	51 %

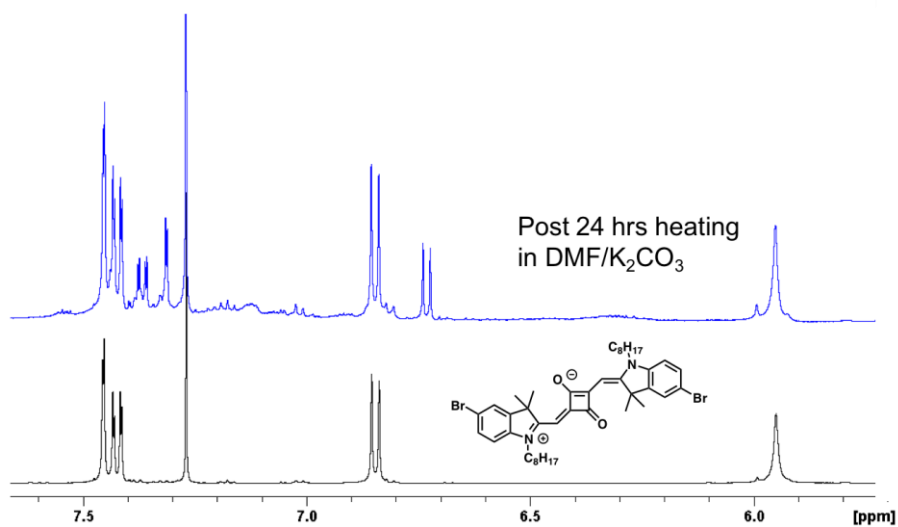
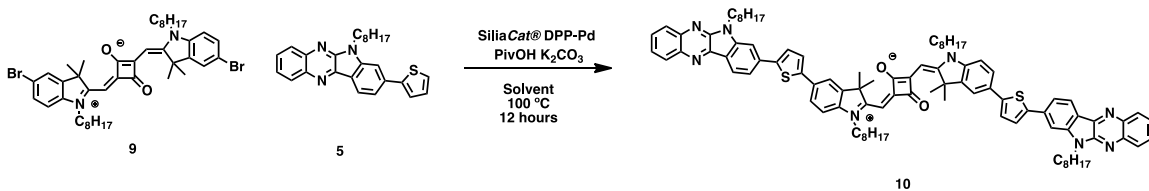


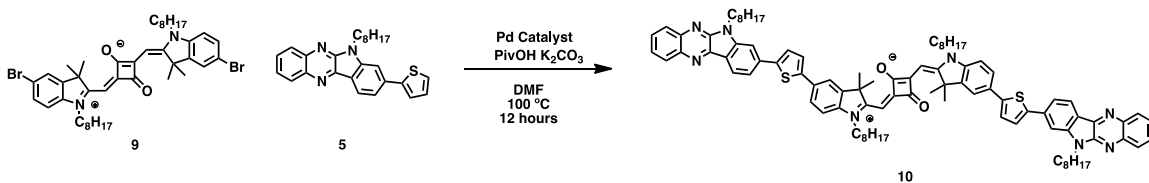
Figure S3. ¹H NMR spectrum of **9** before (bottom) and after (top) heating in DMF at 100 °C with 2 equivalents of K₂CO₃ for 18 hours.

Reactions were repeated at 100 °C for 12 hours varying the solvent.



Solvent	Catalyst	Temperature	Time	Isolated yield
DMA	SiliaCat® DPP-Pd	100 °C	12 hours	55 %
Toluene	SiliaCat® DPP-Pd	100 °C	12 hours	0 %
1,4 dioxane	SiliaCat® DPP-Pd	100 °C	12 hours	0 %
THF	SiliaCat® DPP-Pd	100 °C	12 hours	0 %

Using DMF as the solvent and 12 hours at 100 °C for the reaction time and temperature, various catalyst systems were assessed. A catalyst loading of 10 % was used with three equivalents of the corresponding ligand.



Solvent	Catalyst and Ligand	Temperature	Time	Isolated yield
DMF	Pd(OAc) ₂	100 °C	12 hours	28 % *
DMF	Pd(PPh ₃) ₄	100 °C	12 hours	19 % *
DMF	[Pd(OAc) ₂][P(<i>o</i> -anisole) ₃]	100 °C	12 hours	N/A
DMF	[Pd(OAc) ₂][P(<i>o</i> -tolyl) ₃]	100 °C	12 hours	N/A

*Baseline impurities are present in final product after standard purification procedure. See Figure S4.

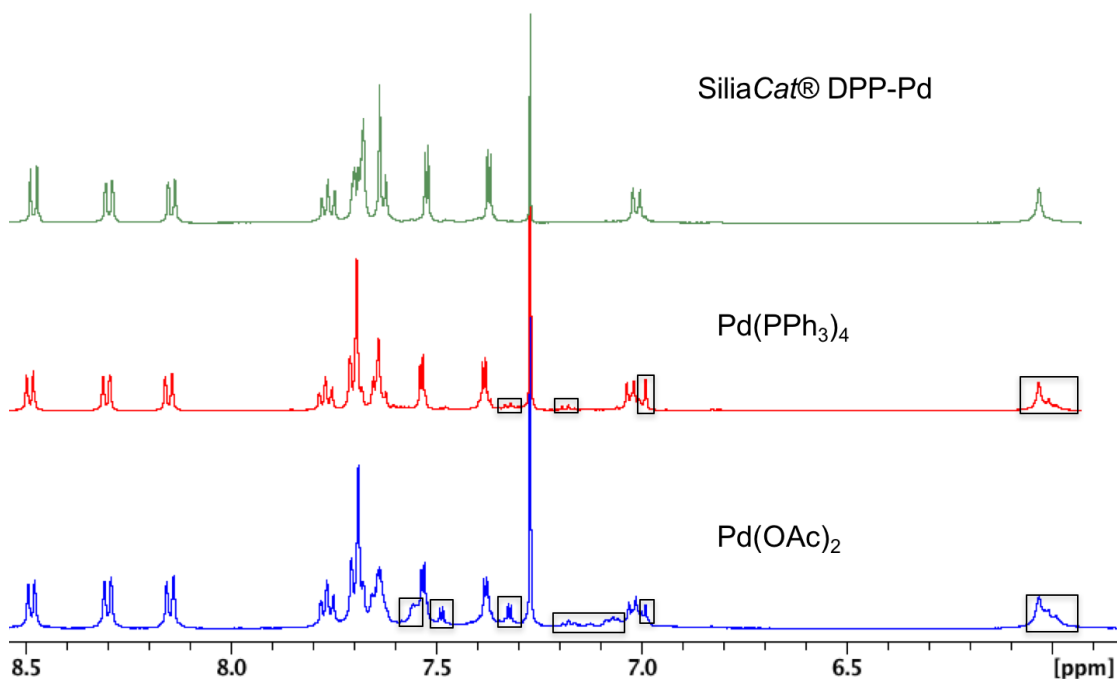
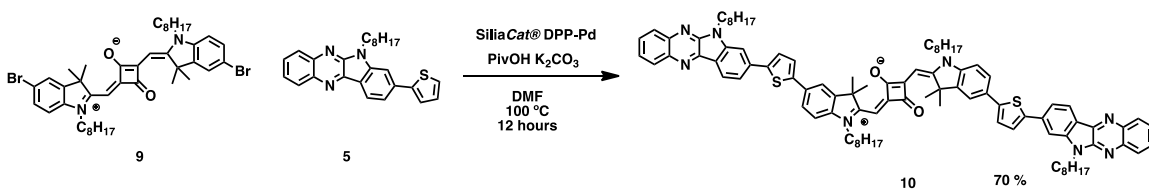


Figure S4. Aromatic region of ^1H NMR spectra of **SIIQ** synthesized using three different Pd catalysts (SiliaCat® DPP-Pd, $\text{Pd}(\text{PPh}_3)_4$, and $\text{Pd}(\text{OAc})_2$). Conditions: DMF solvent, K_2CO_3 , $100\text{ }^\circ\text{C}$, PivOH. The reaction using SiliaCat® DPP-Pd gave the cleanest product as determined by ^1H NMR spectroscopy. Black boxes show unidentifiable impurities.

Using the optimized conditions of 12 hours at $100\text{ }^\circ\text{C}$ in DMF with SiliaCat® DPP-Pd as the catalyst, the reaction was scaled up from 100 mg to 500 mg which was found to lead to higher yield of final product.

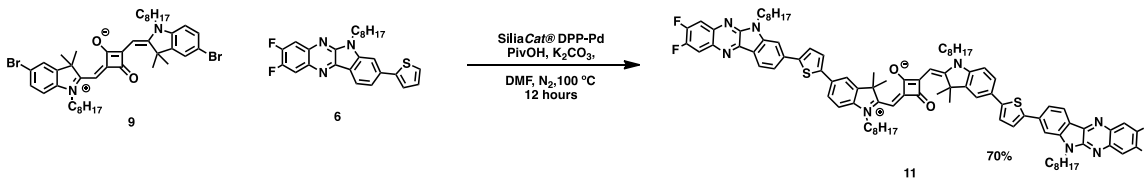
Scale up synthesis of compound 10.



Compound **9** (559 mg, 0.718 mmol), **5** (619 mg, 1.497 mmol), SiliaCat® DPP-Pd (180 mg, 0.045 mmol Pd), pivalic acid (34 mg, 0.33 mmol), and potassium carbonate (247 mg, 1.787 mmol) were added to a 20 mL pressure vial and sealed under N_2 with a Teflon® cap. Anhydrous DMF (10 mL) was syringed into the vessel and the reaction mixture was stirred and heated at $100\text{ }^\circ\text{C}$ in a bead bath for 12 hours. The cooled mixture was poured into MeOH (100 mL) and stirred for two hours. The resulting dark green powder was filtered and washed with MeOH (20 mL). The material was purified by column chromatography using a solvent gradient from petroleum ether to THF with product elution at 100% THF. The solvent was removed under reduced pressure and the resulting material

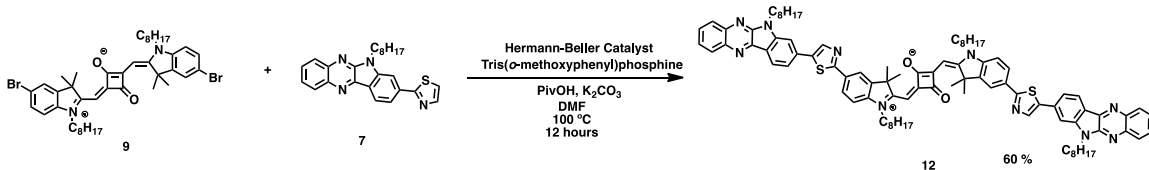
was recrystallized from EtOAc and filtered washing with acetone to yield **10** as a dark green solid (729 mg, 70% yield). $^1\text{H NMR}$ (500 MHz, CDCl_3 , ppm): δ 8.48 (d, $^1J= 7.95$ Hz, 1H), 8.30 (d, $^1J= 8.05$ Hz, 1H), 8.14 (d, $^1J= 8.25$ Hz, 1H) 7.76 (m, 1H), 7.69 (m, ov, 3H), 7.62-7.64 (m, ov, 2H) 7.52 (d, $^1J= 3.70$ Hz, 1H), 7.37 (d, $^1J= 3.75$ Hz, 1H), 7.01 (d, $^1J= 8.70$ Hz, 1H), 6.03 (s, 1H), 4.55 (t, 2H), 4.01 (s, br, 2H), 2.02 (quin, 2H), 1.89 (ov, 8H), 1.22-1.52 (m, ov, 20H), 0.90 (t, 3H), 0.86 (t, 3H) $^{13}\text{C NMR}$ (500 MHz, CDCl_3 , ppm): δ 181.87, 179.04, 168.86, 145.69, 144.45, 143.98, 142.64, 141.69, 140.04, 139.13, 138.94, 136.33, 129.42, 128.68, 128.11, 127.29, 125.48, 124.99, 124.90, 123.43, 122.62, 119.09, 118.07, 118.02, 109.19, 105.38, 86.74, 48.75, 43.38, 40.88, 31.27, 31.20, 28.80, 28.70, 28.63, 27.93, 26.65, 26.59, 26.56, 26.48, 22.06, 13.54. Expected: 94 Found 42. **MS (MALDI-TOF)**: m/z 1443.79 calcd. 1443.80.

Synthesis of compound 11.



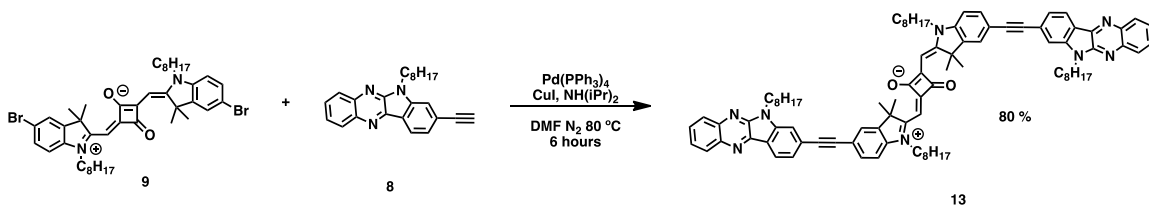
Compound **11** was synthesized following the optimized DHA procedure for compound **10**. The resulting material was purified by column chromatography using a gradient from hexanes to DCM with product elution using 1% (V/V) trimethylamine/DCM. The material was then recrystallization from ethyl acetate followed by ethanol, yielding **11** as a dark green solid (70% yield). $^1\text{H NMR}$ (500 MHz, CDCl_3 , ppm): δ 8.41(d, $^1J= 8.05$ Hz, 1H), 7.99 (dd, $^1J= 8.45$ Hz, $^2J= 2.45$ Hz, 1H), 7.84 (dd, $^1J= 8.20$ Hz, $^2J= 2.85$ Hz, 1H), 7.67 (dd, $^1J= 1.35$ Hz, $^2J= 6.75$ Hz, 1H) 7.61-7.64 (m, ov, 3H) 7.51 (d, $^1J= 3.75$ Hz, 1H), 7.36 (d, $^1J= 3.75$ Hz, 1H), 7.02 (d, $^1J= 8.80$ Hz, 1H), 6.03 (s, 1H), 4.50 (t, 2H), 4.02 (s, br, 2H), 1.99 (quin, 2H), 1.89 (m, ov, 8H), 1.23-1.50 (m, ov, 20H), 0.90 (t, 3H), 0.86 (t, 3H) $^{19}\text{F NMR}$ (500 MHz, DMSO- d_6 , ppm) δ -133.240 (d, $^1J= 23.00$ Hz) -136.983 (d, $^1J= 23.05$ Hz). $^{13}\text{C NMR}$ (500 MHz, CDCl_3 , ppm): δ 179.09, 168.87, 145.61, 145.59, 144.23, 144.15, 142.36, 141.74, 139.13, 139.11, 137.04 (d $^3J_{\text{C-F}}=10.63$ Hz), 136.60, 135.49 (d $^3J_{\text{C-F}}=10.42$ Hz), 129.34, 125.01, 123.43, 122.63, 119.09, 118.27, 117.51, 114.08 (d $^2J_{\text{C-F}}= 19.45$ Hz), 112.82 (d $^2J_{\text{C-F}}= 17.67$ Hz), 109.19, 105.35, 86.77, 48.74, 43.39, 40.94, 31.25, 31.20, 28.79, 28.67, 28.62, 27.90, 26.64, 26.59, 26.56, 26.46, 22.06, 13.53. Expected: 94 Found 40. **MS (MALDI-TOF)**: m/z 1514.75 calcd. 1514.75.

Synthesis of compound 12.



Compound **9** (100 mg, 0.128 mmol), **7** (112 mg, 0.270 mmol), *trans*-Bis(acetato)bis[*o*-(*di*-*o*-tolylphosphino)benzyl]dipalladium(II) (Hermann-Beller catalyst) (20 mg, 0.0213 mmol), tris(*o*-methoxyphenyl)phosphine (15 mg, 0.0425 mmol), pivalic acid (4 mg, 0.39 mmol), and potassium carbonate (33 mg, 0.239 mmol) were added to a 10 mL pressure vial and sealed under N₂ with a Teflon® cap. Anhydrous DMF (2 mL) was syringed into the vessel and the reaction mixture was stirred and heated at 100 °C in a bead bath for 12 hours. The cooled mixture was poured into MeOH (100 mL) and stirred for two hours. The resulting dark green powder was filtered and washed with MeOH (20 mL). The material was subsequently dissolved in DCM and rinsed through a silica plug with DCM/THF to remove the inorganics. Upon solvent removal, the material was stirred and heated in acetone for 3 hours followed by hot filtration washing with acetone. The material was then recrystallization from DMSO and filtered washing with methanol to yield **12** as a shiny green/gold solid (110 mg, 0.076 mmol 60% yield). ¹H NMR (500 MHz, CDCl₃, ppm): δ 8.49 (d, ¹J=7.95 Hz, 1H), 8.29 (d, ¹J=8.05 Hz, 1H), 8.19 (s, 1H), 8.13 (d, ¹J=8.2 Hz, 1H), 8.01 (s, 1H), 7.92 (d, ¹J=8.1 Hz, 1H), 7.76 (t, 1H), 7.69 (t, 1H), 7.64 (d, ¹J=8.25 Hz), 7.61 (s, 1H), 7.00 (d, ¹J=8.3 Hz, 1H), 6.06 (s, 1H), 4.54 (t, 2H), 3.97 (s, br, 2H), 2.01 (quin, 2H), 1.91, (s, 6H), 1.84 (m, 2H), 1.50-1.35 (m, ov, 8H), 1.35-1.21 (m, ov, 12H), 0.90 (t, 3H), 0.86 (t, 3H). ¹³C NMR (500 MHz, CDCl₃, ppm): δ 180.16, 169.21, 166.85, 145.58, 144.26, 143.59, 142.64, 140.13, 139.63, 138.96, 138.83, 138.44, 133.28, 128.73, 128.70, 128.32, 127.33, 126.22, 125.62, 122.78, 119.66, 118.82, 118.68, 109.07, 106.46, 87.36, 48.72, 43.42, 40.93, 31.25, 31.19, 28.77, 28.69, 28.62, 27.93, 26.62, 26.57, 26.54, 26.48, 22.06, 13.54 Expected: 92 Found: 41. MS (MALDI-TOF): *m/z* 1444.78. calcd. 1444.78.

Synthesis of compound 13.



Compound **9** (253 mg, 0.325 mmol), **8** (255 mg, 0.717 mmol), Pd(PPh₃)₄ (25 mg, 0.022 mmol), and CuI (15 mg, 0.08 mmol) were added to a 10 mL pressure vial and sealed under N₂ with a Teflon® cap. Anhydrous DMF (12 mL) and NH(*i*Pr)₂ (1 mL) was syringed into the vessel and the reaction mixture was stirred and heated at 80 °C in a bead bath for 6 hours. The cooled mixture was poured into MeOH (60 mL) and stirred overnight. The resulting material was filtered and washed with MeOH (20 mL). The material was subsequently dissolved in DCM/THF and sent through a short silica plug to remove

inorganics. The solvent was removed and the shiny green/gold material was slurried in MeOH and filtered and dried under vacuum (345 mg, 0.260 mmol 80% yield). **¹H NMR** (500 MHz, CDCl₃, ppm): δ 8.49 (d, ¹J= 9.95 Hz, 1H), 8.33 (d, ¹J= 9.35 Hz, 1H), 8.17 (d, ¹J= 9.60 Hz, 1H) 7.79 (m, 1H), 7.71 (m, 1H), 7.67-7.58 (m, ov, 4H) 7.02 (d, ¹J= 10.2 Hz, 1H), 6.06 (s, 1H), 4.53 (t, 2H), 4.04 (s, br, 2H), 2.03 (quin, 2H), 1.88 (m, ov, 8H), 1.24-1.52 (m, ov, 20H), 0.92 (t, 3H), 0.89 (t, 3H) **¹³C NMR** (500 MHz, CDCl₃, ppm): δ 180.00, 169.11, 145.60, 143.55, 142.15, 140.19, 138.84, 138.82 131.39, 128.74, 128.40, 127.34, 125.62, 125.12, 125.06, 123.75, 122.08, 118.50, 117.37, 111.68, 108.88, 91.27, 89.88, 87.08 48.58, 43.39, 41.00, 31.25, 31.18, 28.77, 28.71, 28.63, 28.61, 27.91, 26.57, 26.54, 26.49, 22.05, 13.53. Expected: 90 Found: 39. **MS (MALDI-TOF):** *m/z* 1326.81. calcd. 1326.81.

NMR Spectra

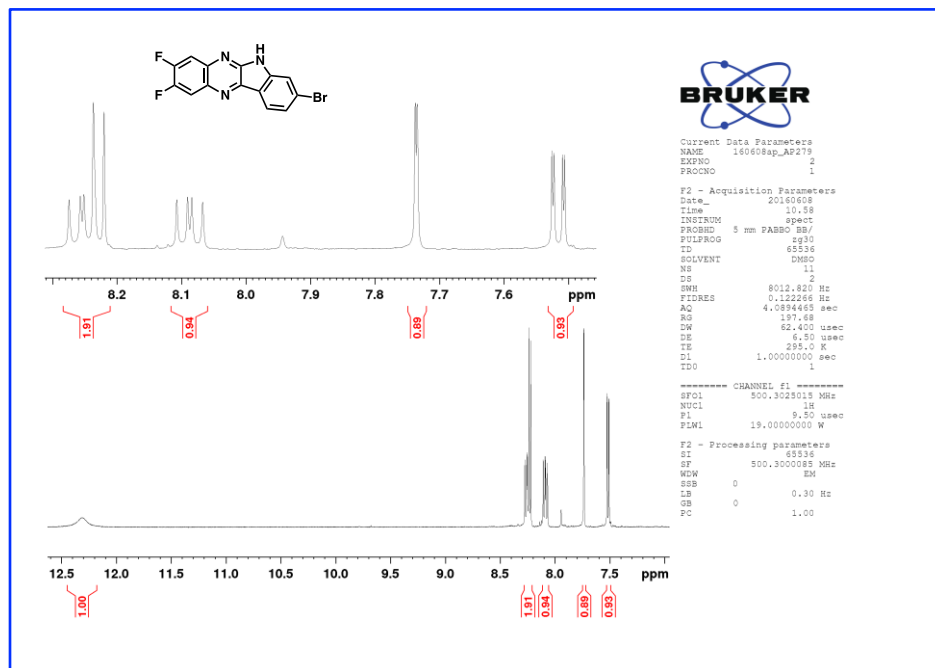


Figure S5. ^1H NMR spectrum of **2** in $\text{DMSO-}D_6$.

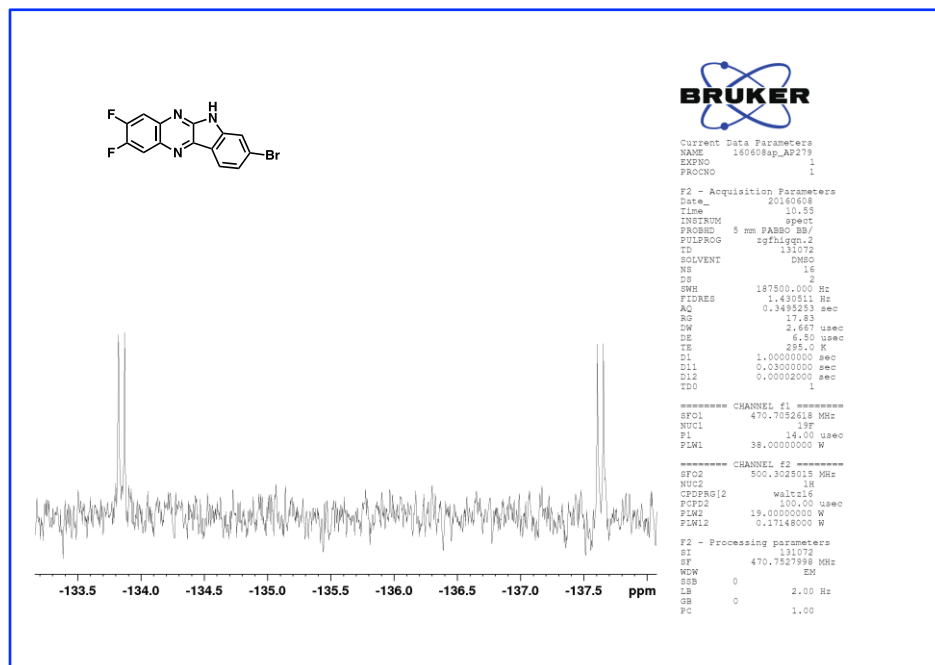


Figure S6. ^{19}F NMR spectrum of **2** in $\text{DMSO-}D_6$.

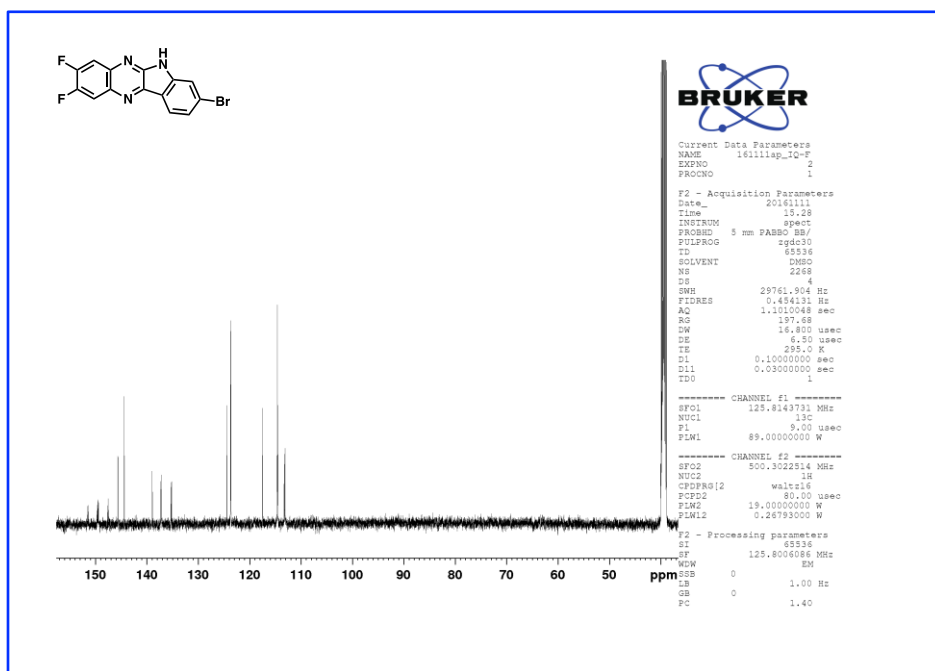


Figure S7. ^{13}C NMR spectrum of **2** in DMSO-D_6

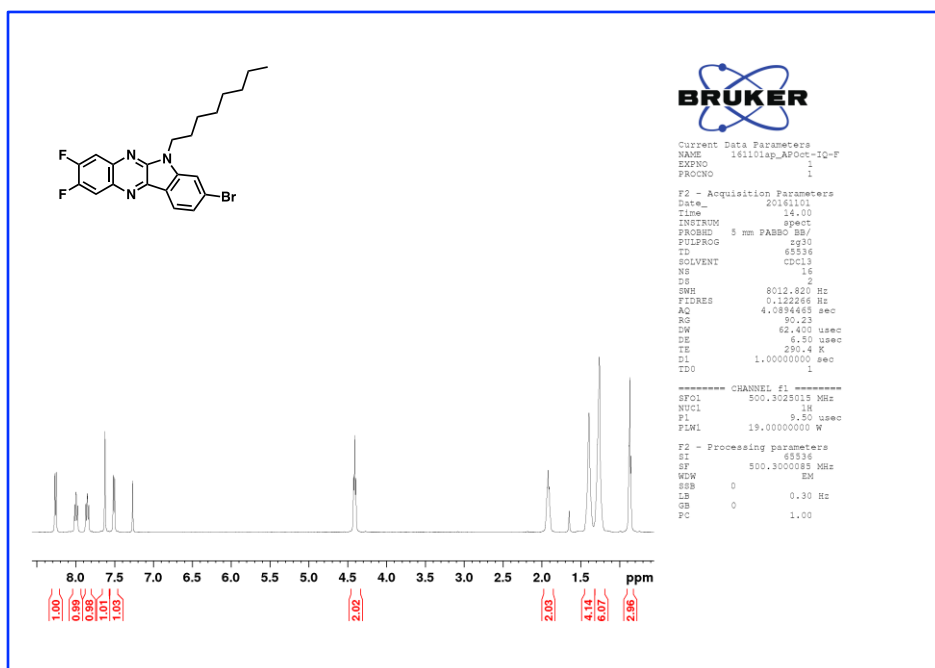


Figure S8. ^1H NMR spectrum of **4** in CDCl_3 .

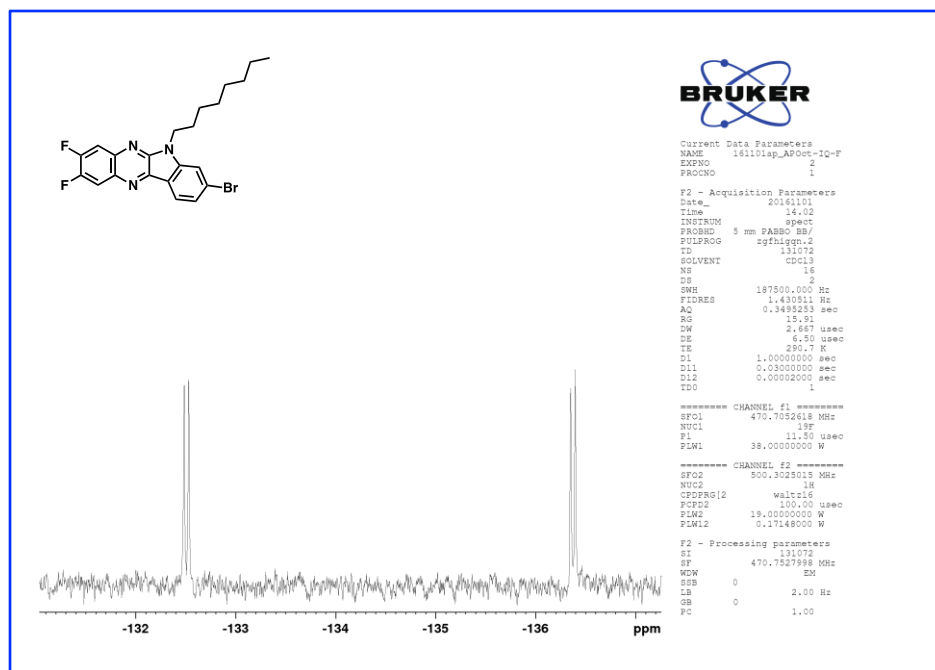


Figure S9. ^{19}F NMR spectrum of **4** in CDCl_3 .

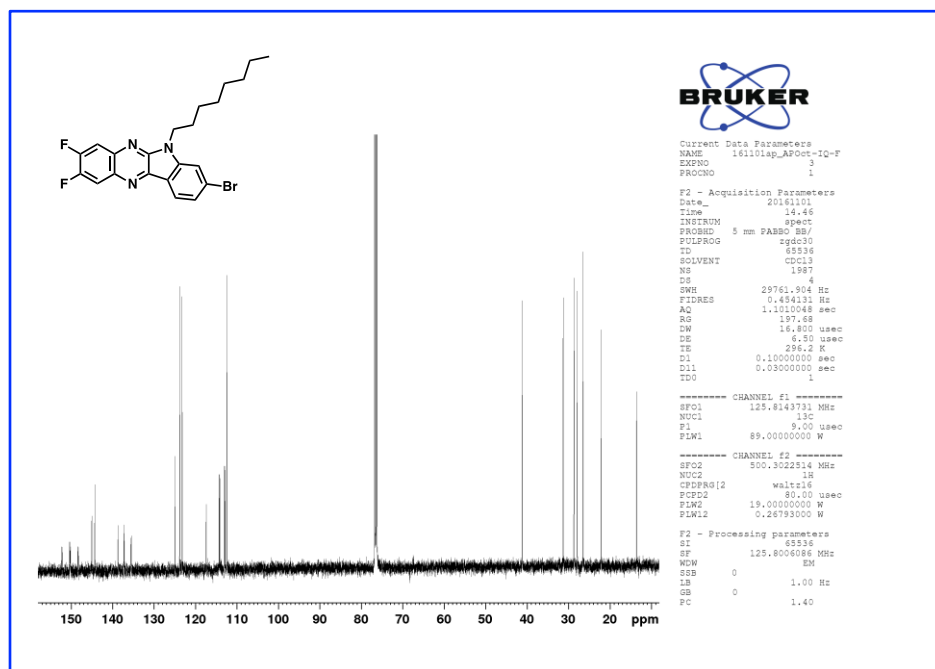


Figure S10. ^{13}C NMR spectrum of **4** in CDCl_3 .

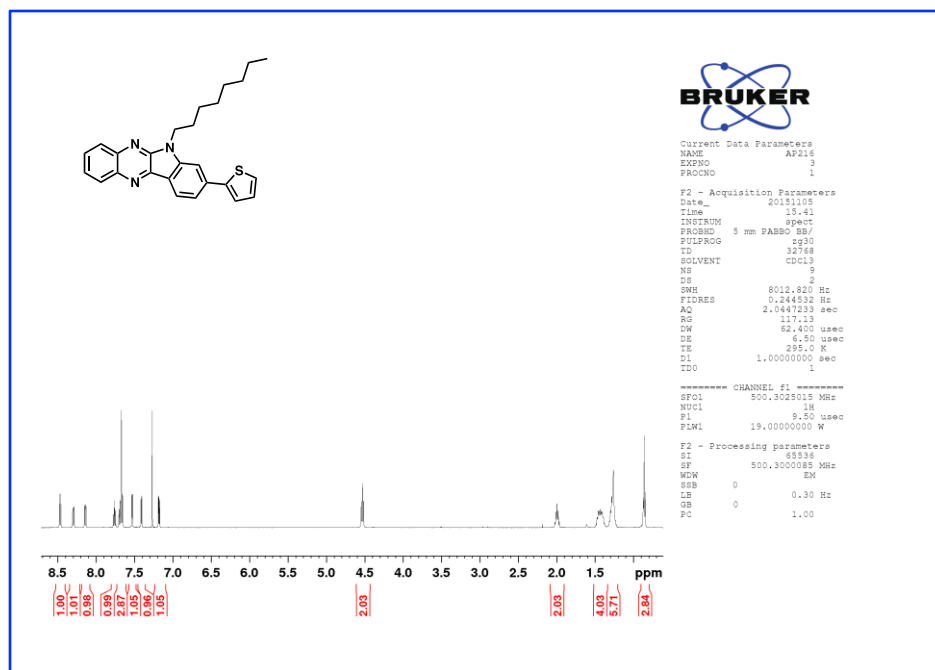


Figure S11. ^1H NMR spectrum of **5** in CDCl_3 .

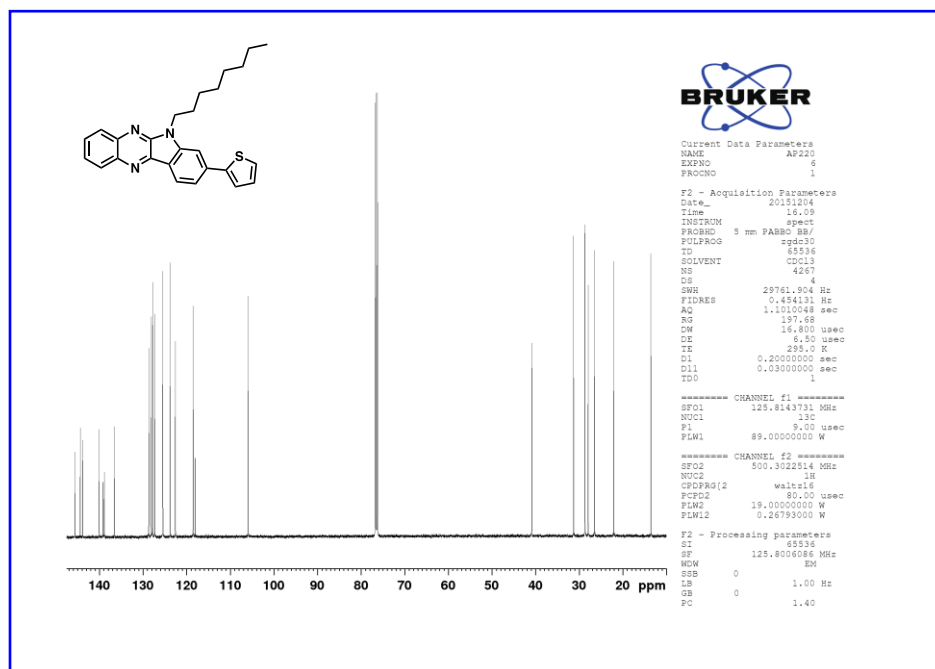


Figure S12. ^{13}C NMR spectrum of **5** in CDCl_3

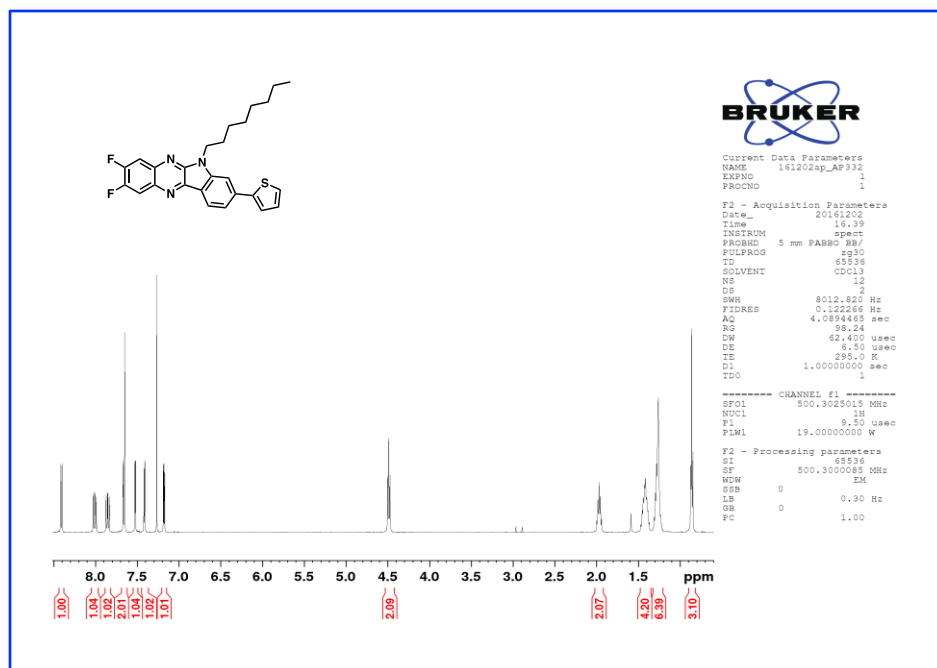


Figure S13. ^1H NMR spectrum of **6** in CDCl_3 .

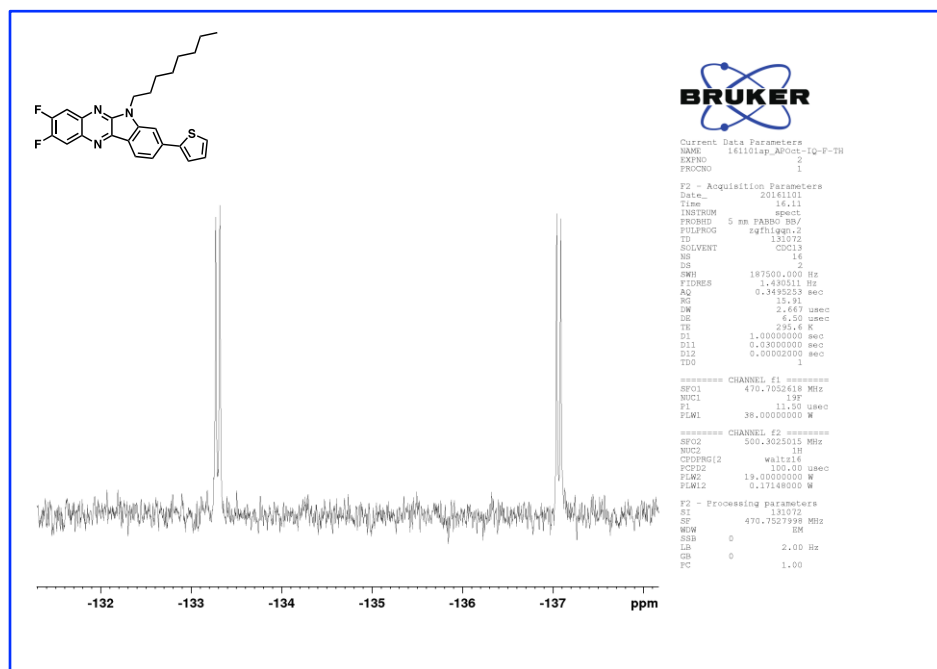


Figure S14. ^{19}F NMR spectrum of **6** in CDCl_3 .

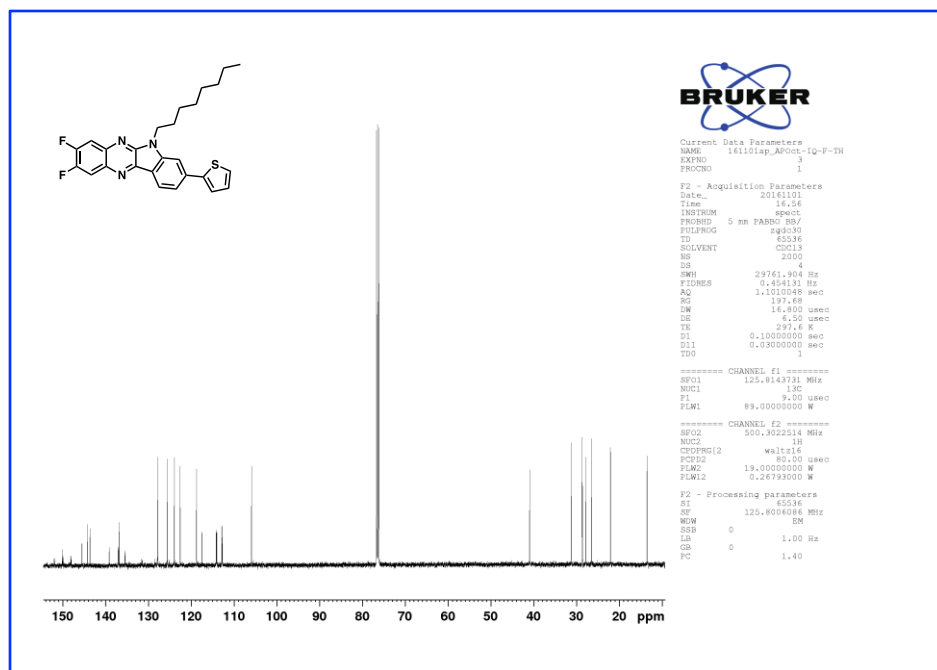


Figure S15. ^{13}C NMR spectrum of **6** in CDCl_3 .

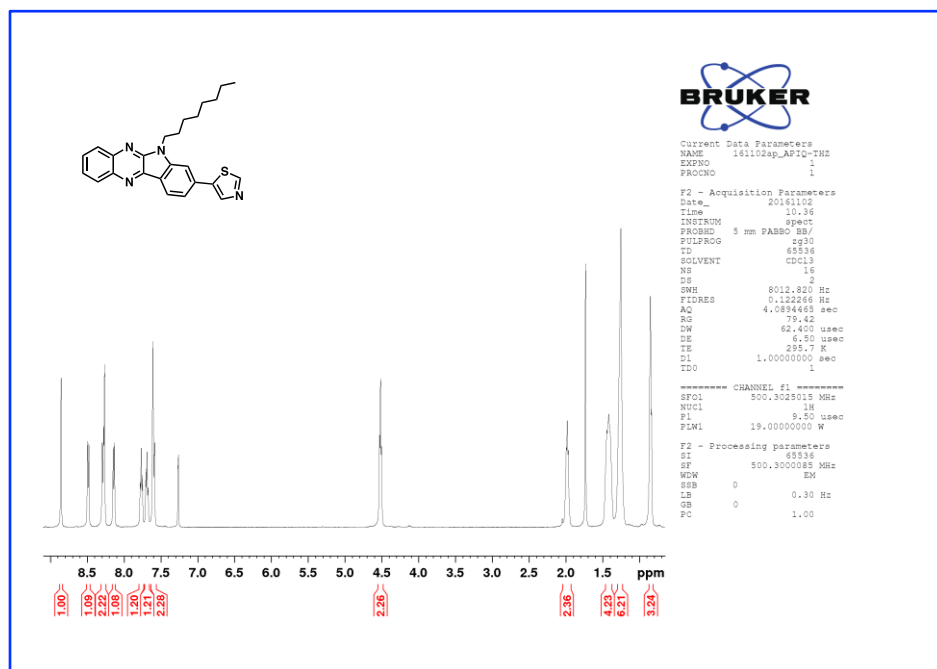


Figure S16. ^1H NMR spectrum of **7** in CDCl_3 .

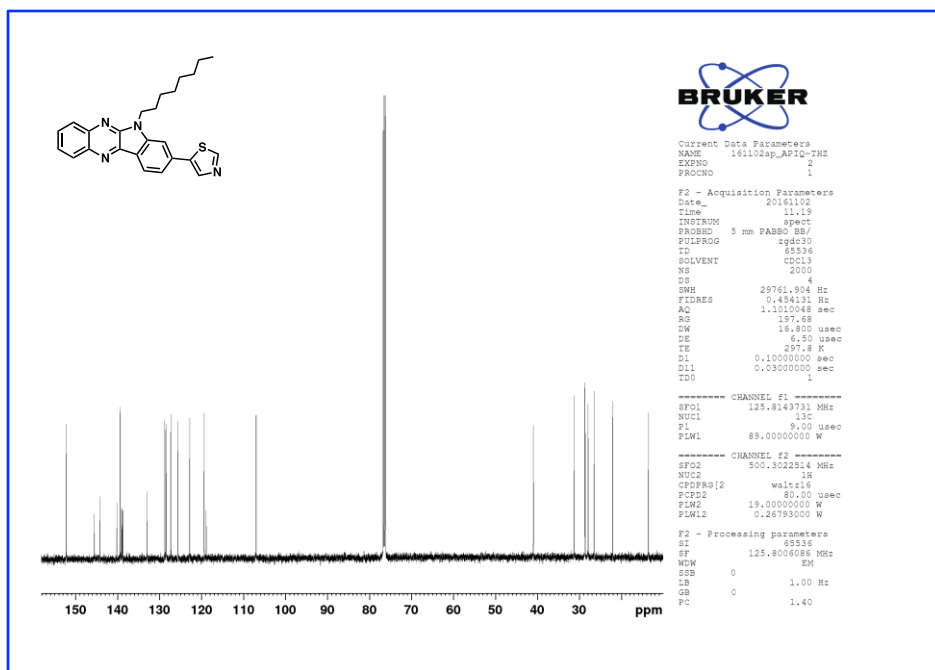


Figure S17. ^{13}C NMR spectrum of **7** in CDCl_3 .

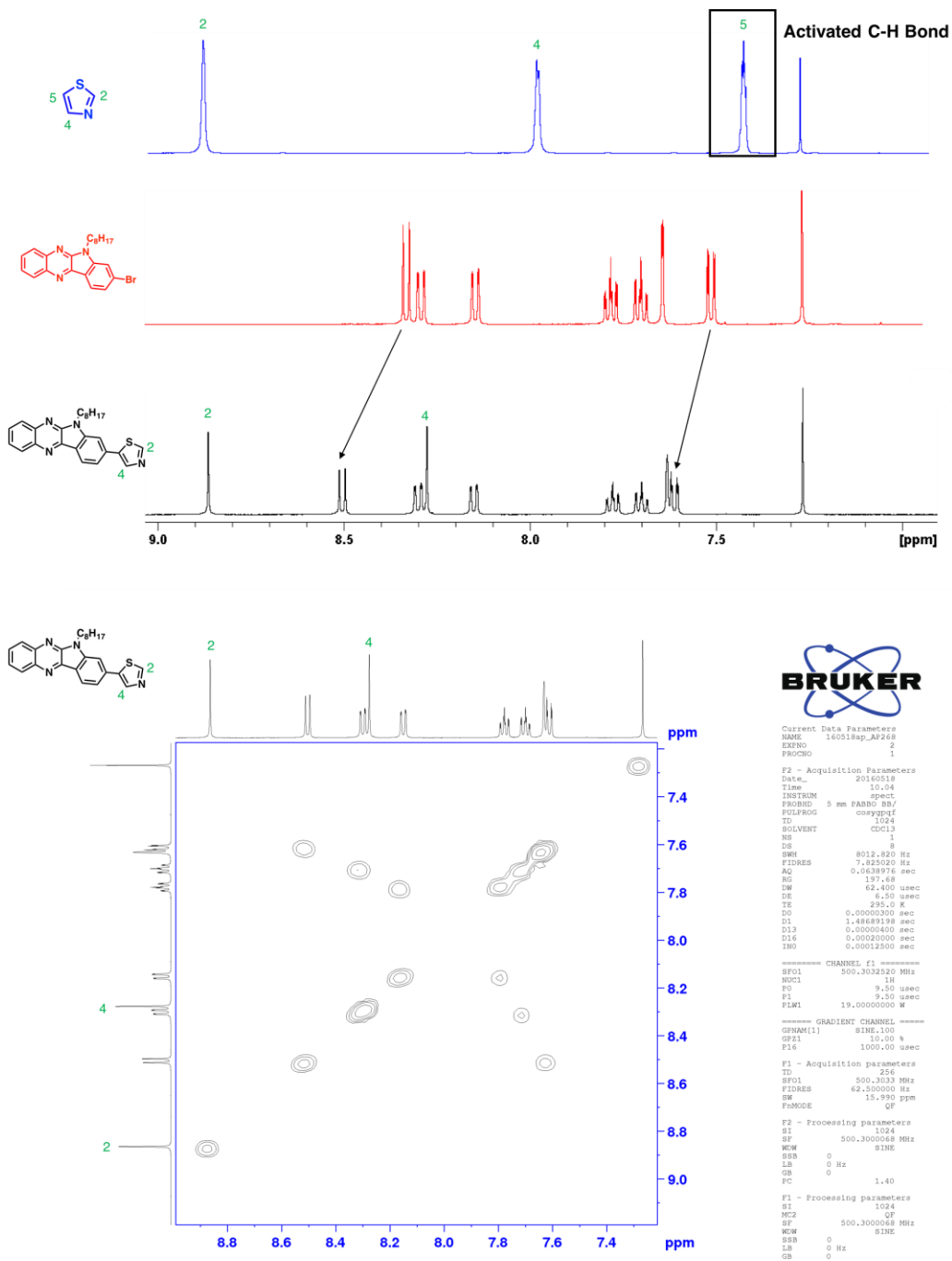


Figure S18. Confirmation of electrophilic substitution onto the 5 position of thiazole.

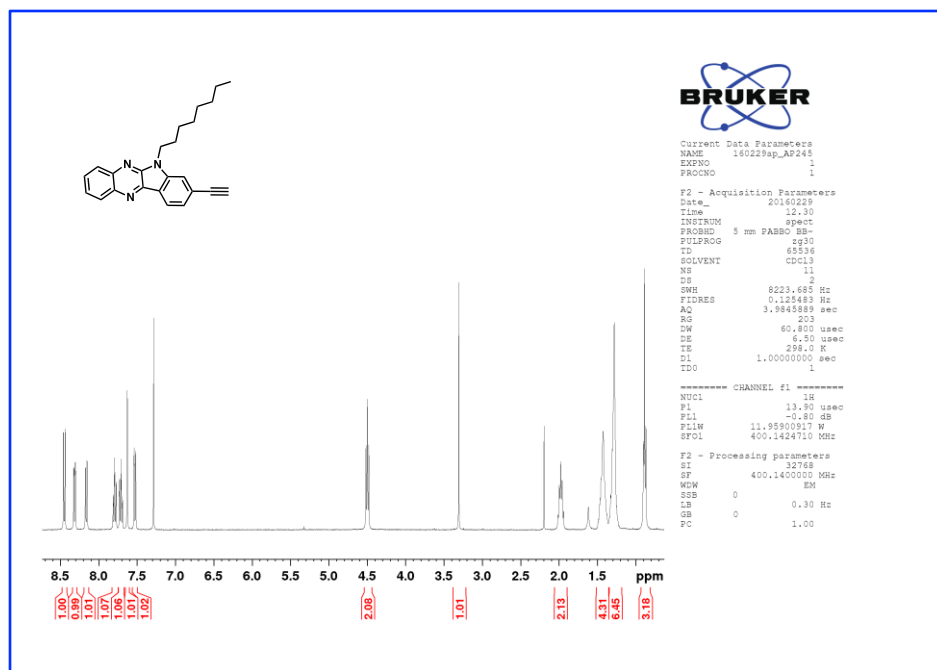


Figure S19. ^1H NMR spectrum of **8** in CDCl_3 .

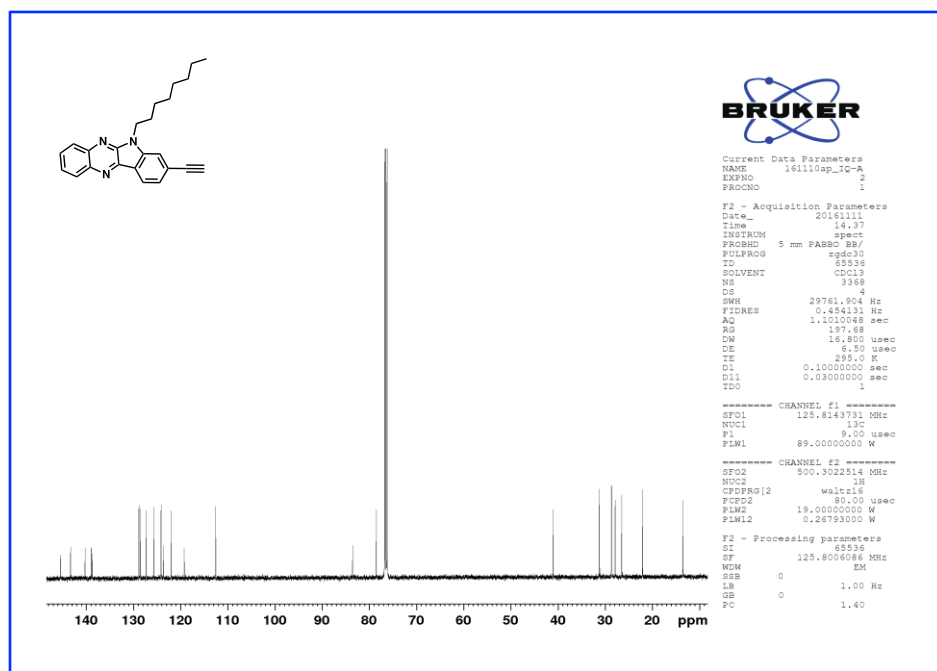


Figure S20. ^{13}C NMR spectrum of **8** in CDCl_3 .

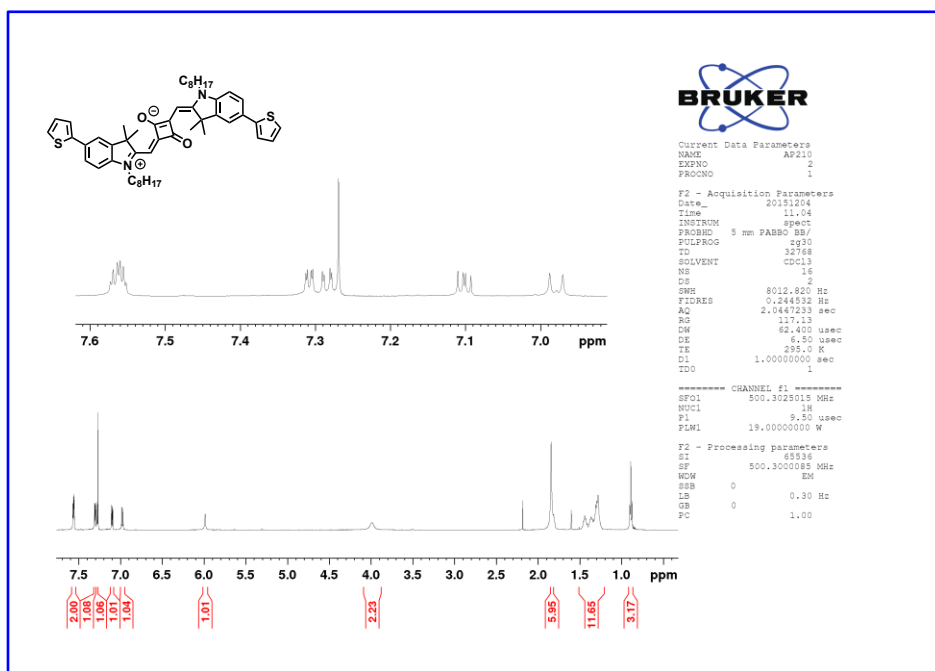


Figure S21. ^1H NMR spectra of **9Th** in CDCl_3 .

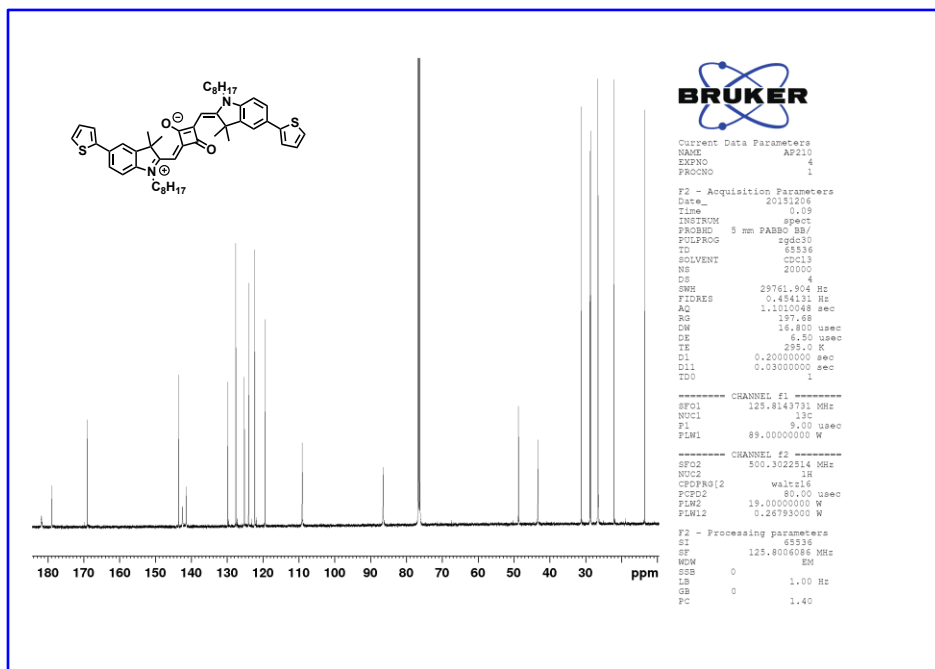


Figure S22. ^{13}C NMR spectra of **9Th** in CDCl_3 .

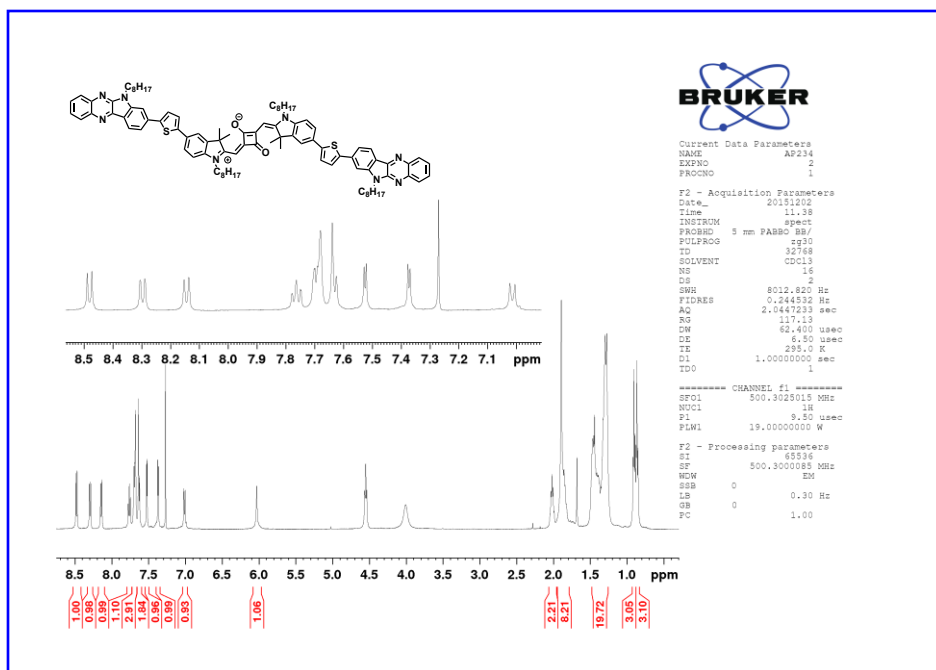


Figure S23. ^1H NMR spectrum of **10** in CDCl_3 .

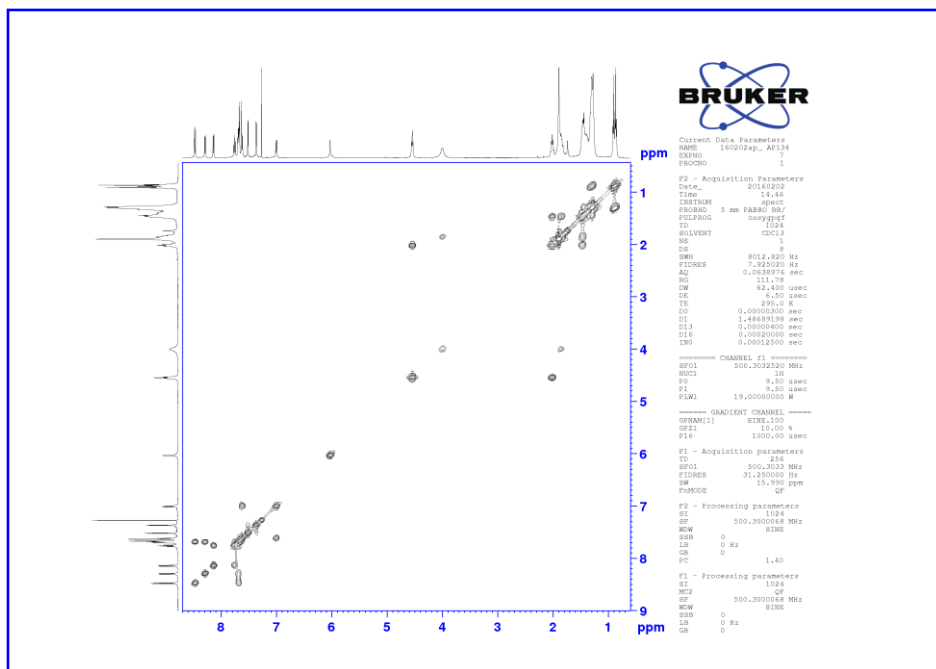


Figure S24. 2D ^1H - ^1H COSY NMR spectrum of **10** in CDCl_3 .

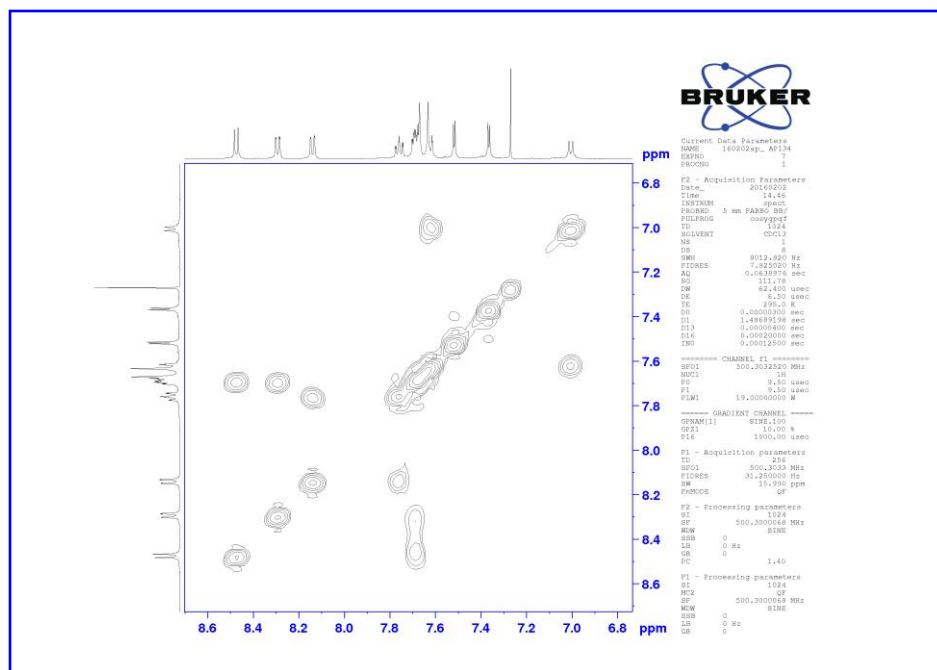


Figure S25. 2D ^1H - ^1H COSY NMR spectrum of **10** in CDCl_3 aromatic region.

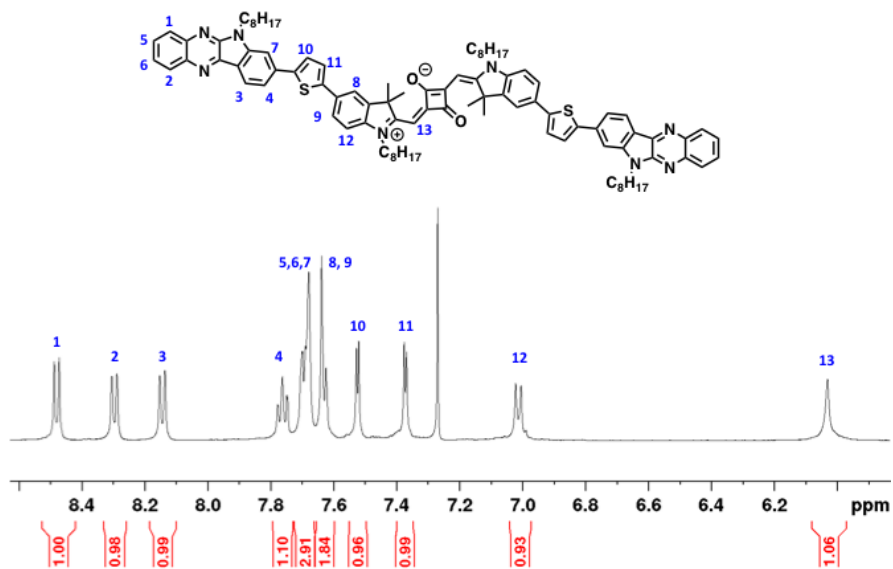


Figure S26. ^1H NMR spectrum of **10** in CDCl_3 assigned aromatic peaks.

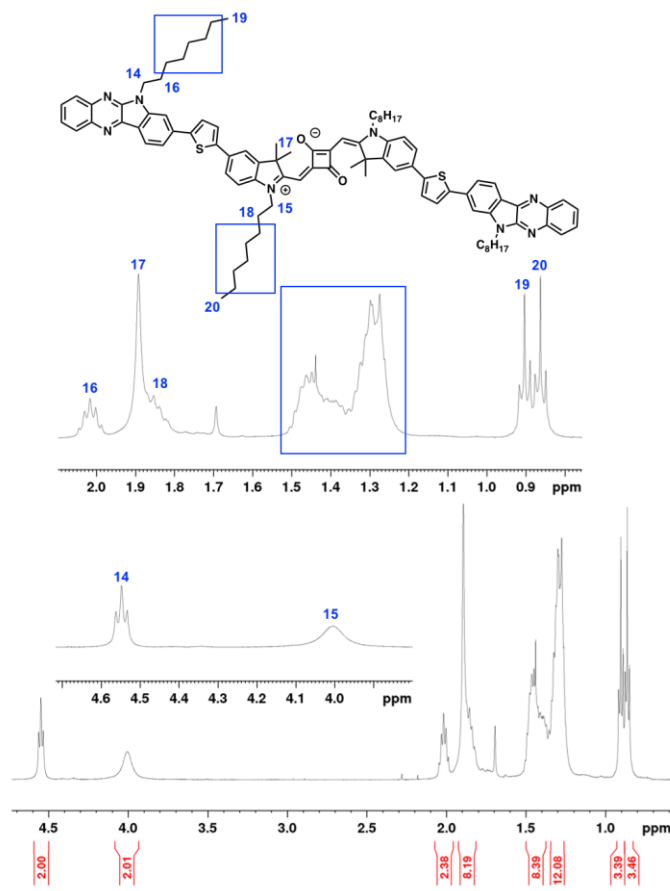
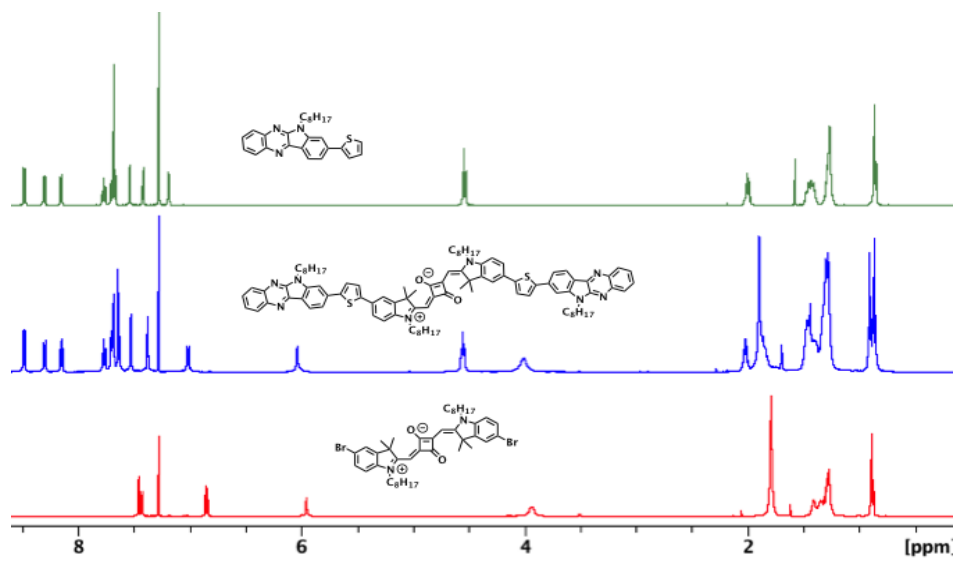


Figure S27. ^1H NMR spectrum of **10** in CDCl_3 assigned aliphatic peaks.



Activated CH bond

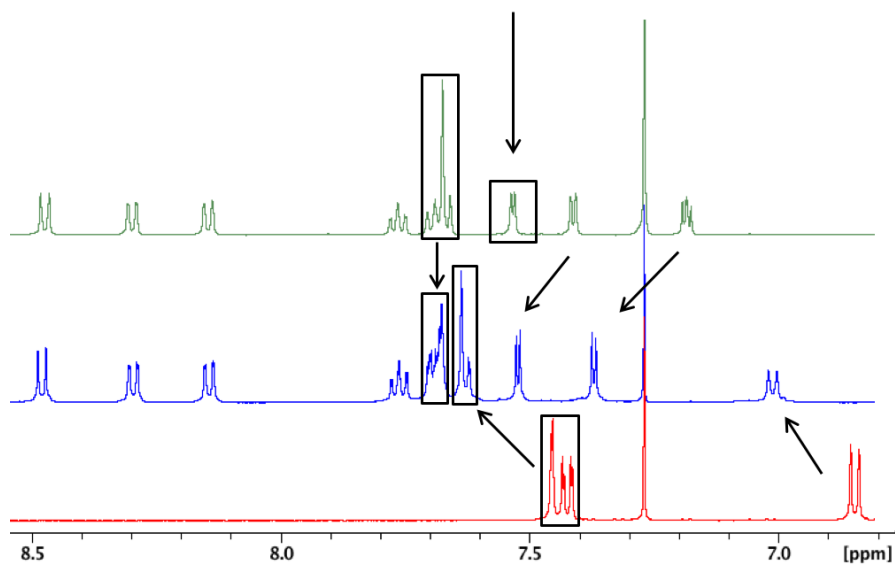


Figure S28. ^1H NMR spectrum of **5**, **9** and **10** in CDCl_3 .

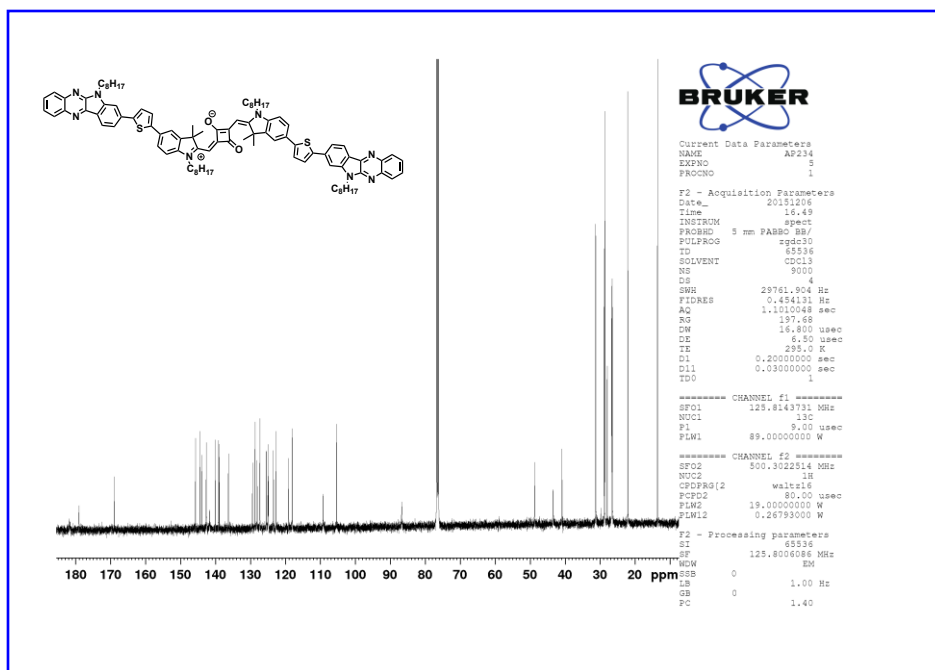


Figure S29. ^{13}C NMR spectra of **10** in CDCl_3

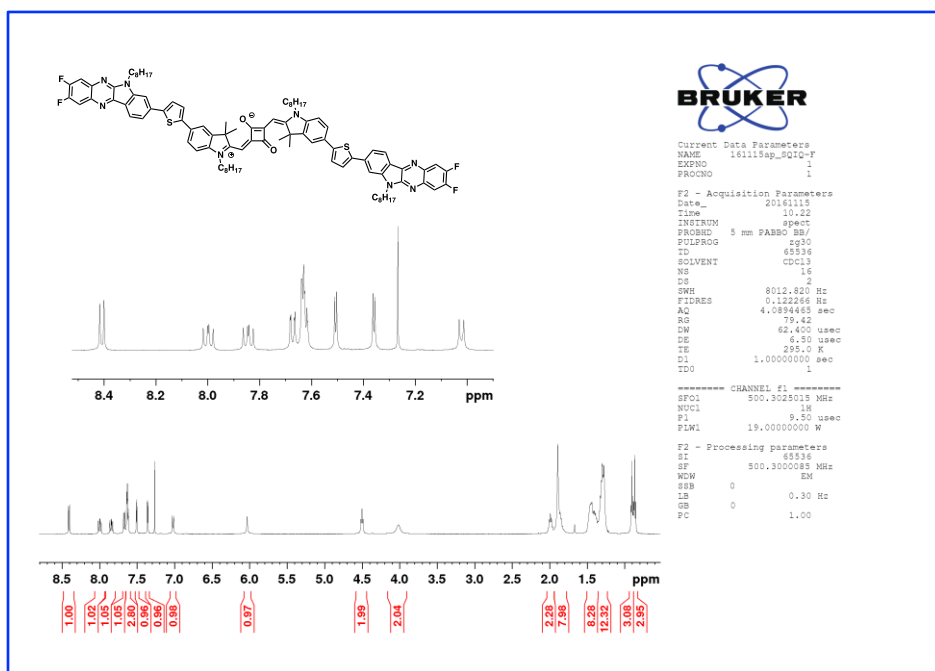


Figure S30. ^1H NMR spectra of **11** in CDCl_3 .

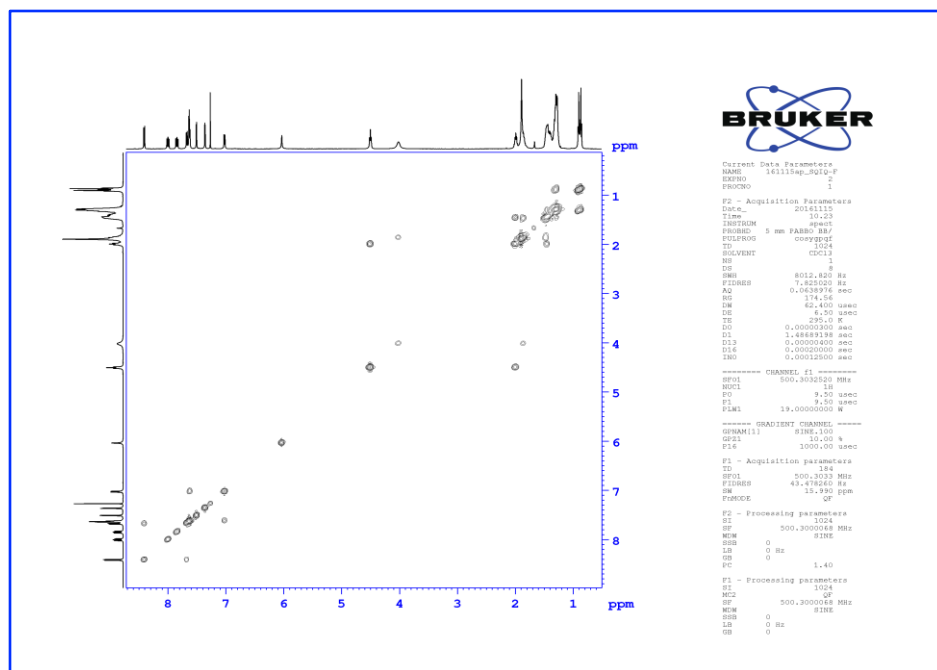


Figure S31. 2D ^1H - ^1H COSY NMR spectrum of **11** in CDCl_3 .

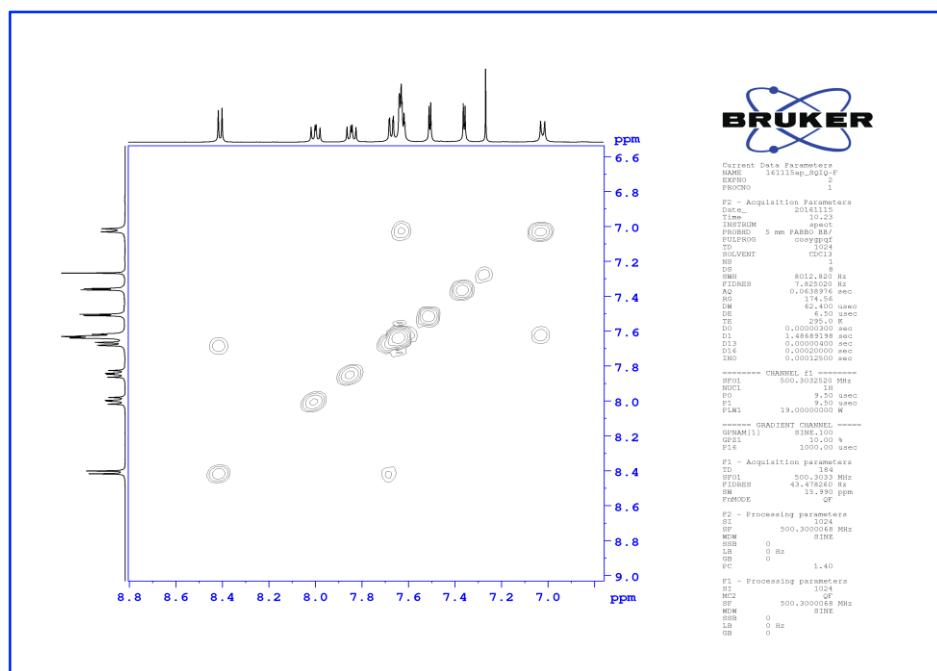


Figure S32. 2D ^1H - ^1H COSY NMR spectrum of **11** in CDCl_3 aromatic region.

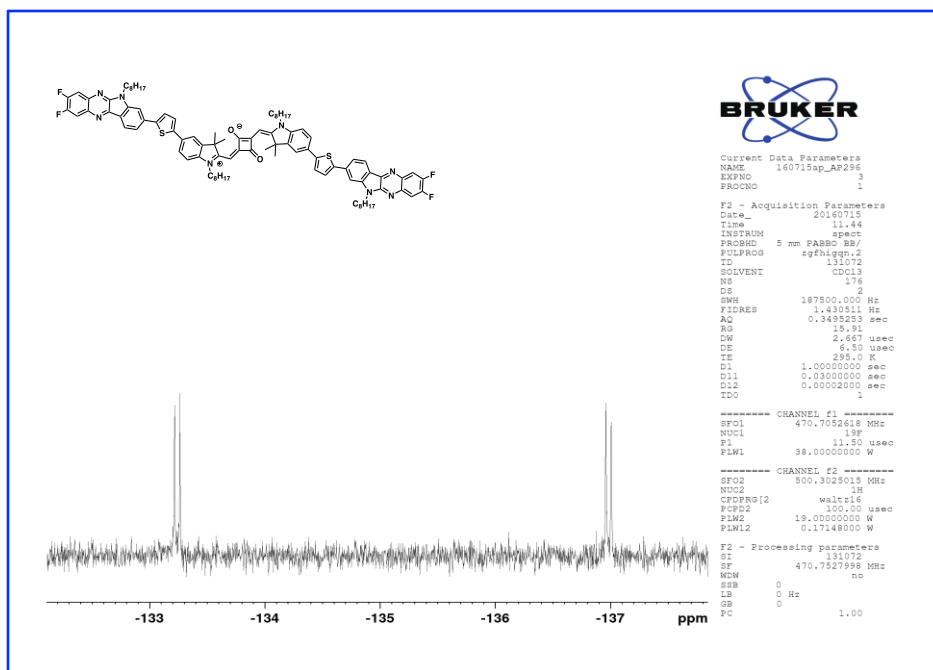


Figure S33. ¹⁹F NMR spectra of **11** in CDCl₃.

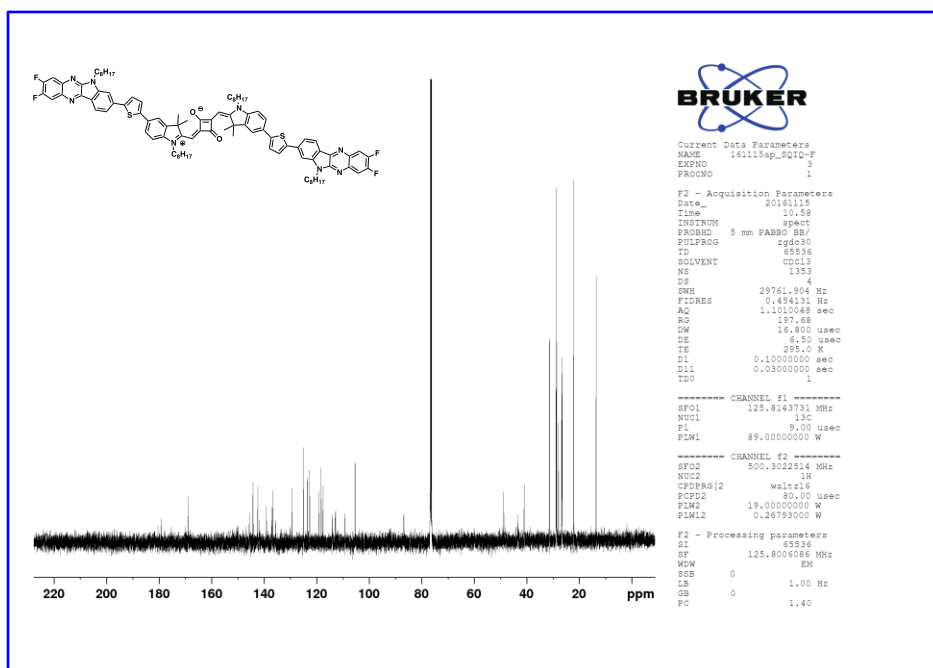


Figure S34. ¹³C NMR spectra of **11** in CDCl₃

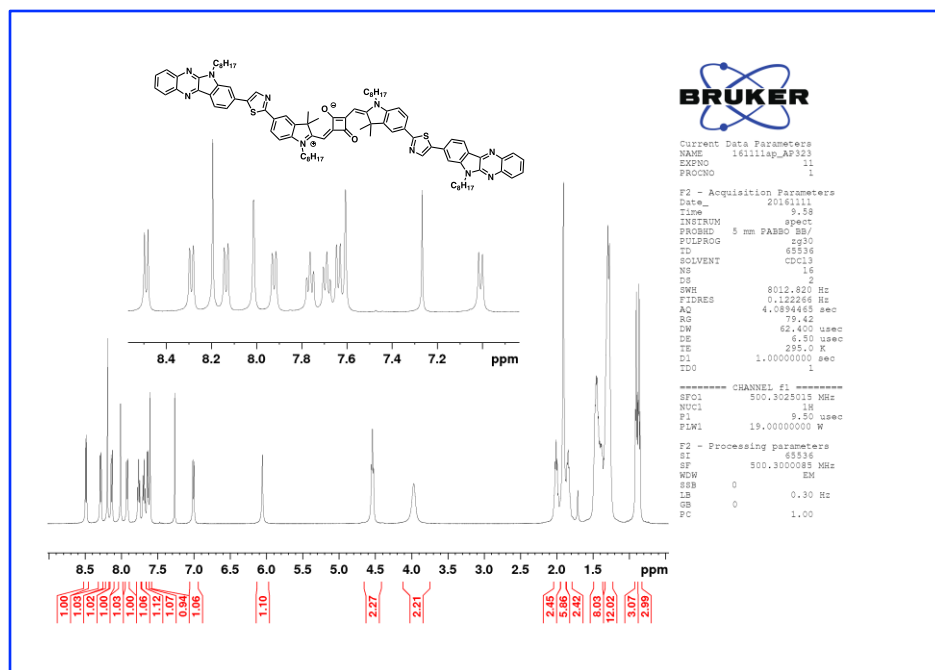


Figure S35. ^1H NMR spectra of **12** in CDCl_3

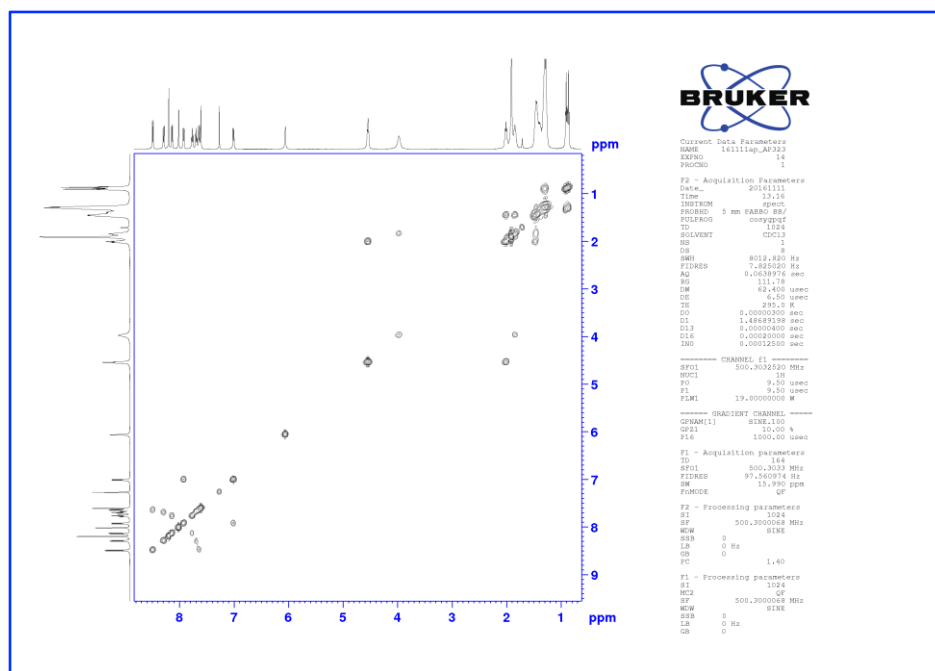


Figure S36. 2D ^1H - ^1H COSY NMR spectrum of **12** in CDCl_3 .

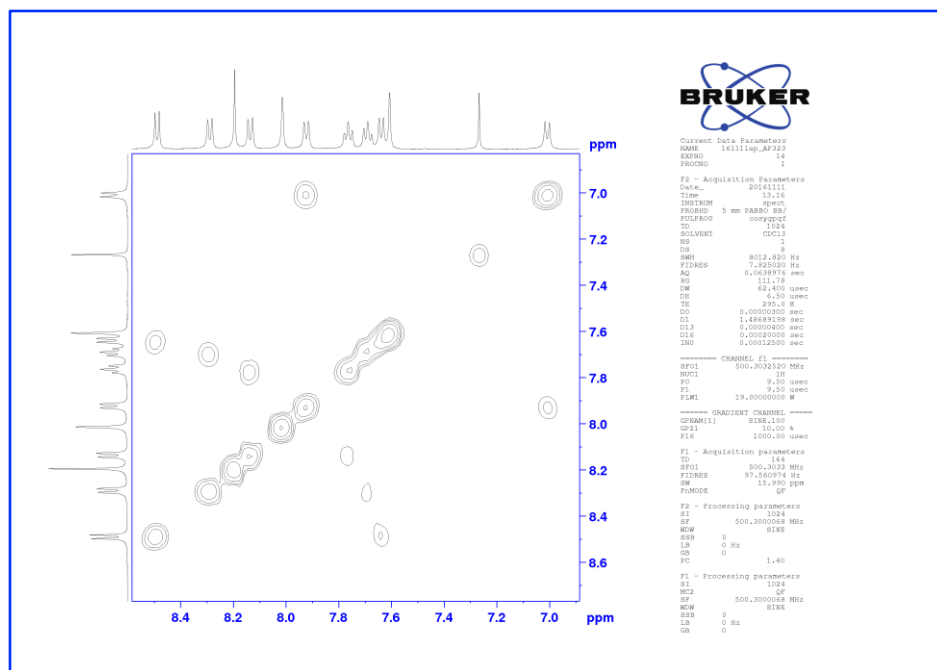


Figure S37. 2D ^1H - ^1H COSY NMR spectrum of **12** in CDCl_3 aromatic region.

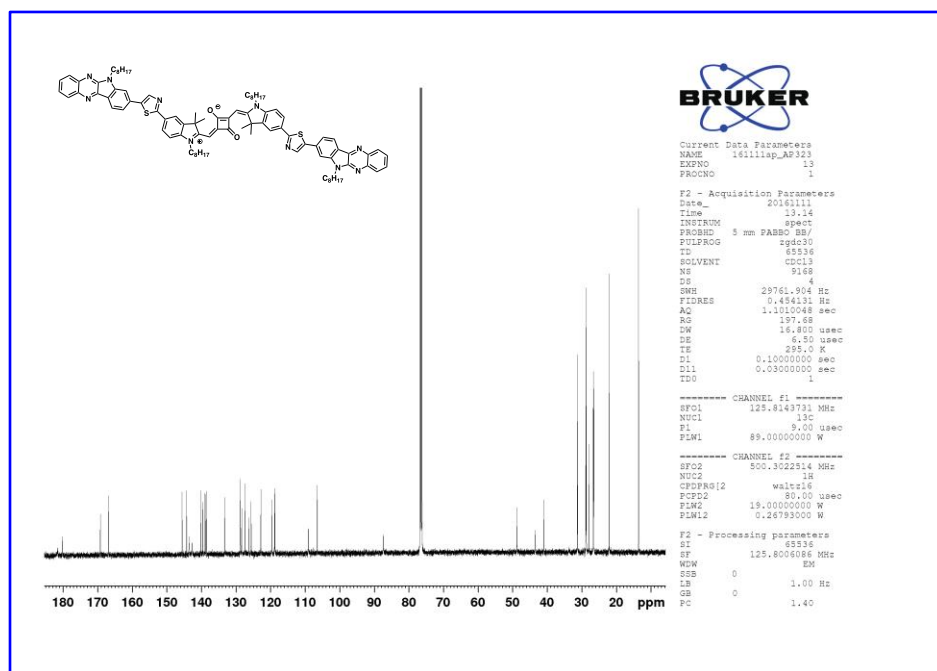


Figure S38. ^{13}C NMR spectra of **12** in CDCl_3

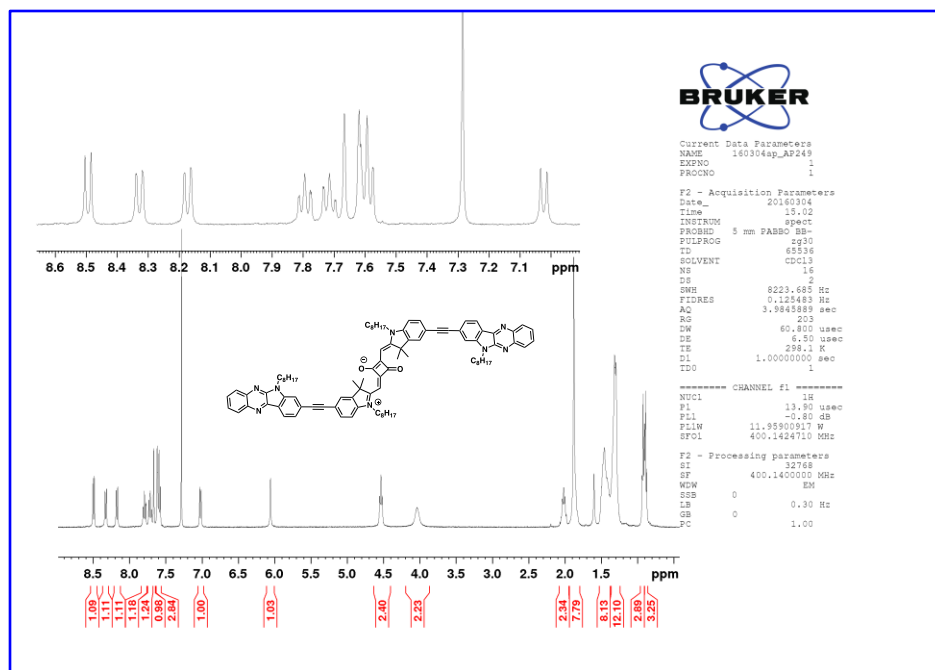


Figure S39. ^1H NMR spectra of **13** in CDCl_3

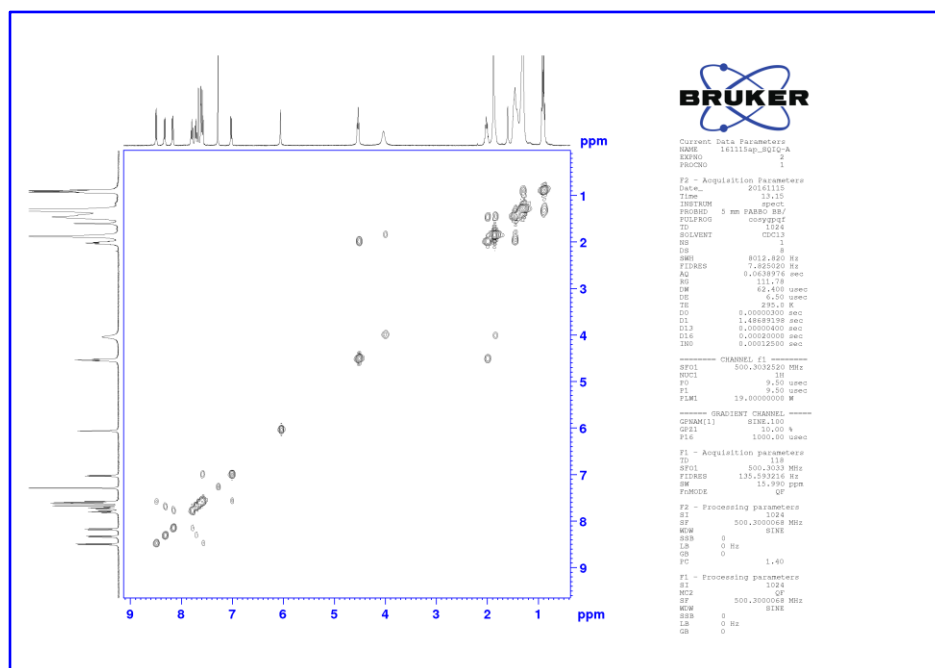


Figure S40. 2D ^1H - ^1H COSY NMR spectrum of **13** in CDCl_3 .

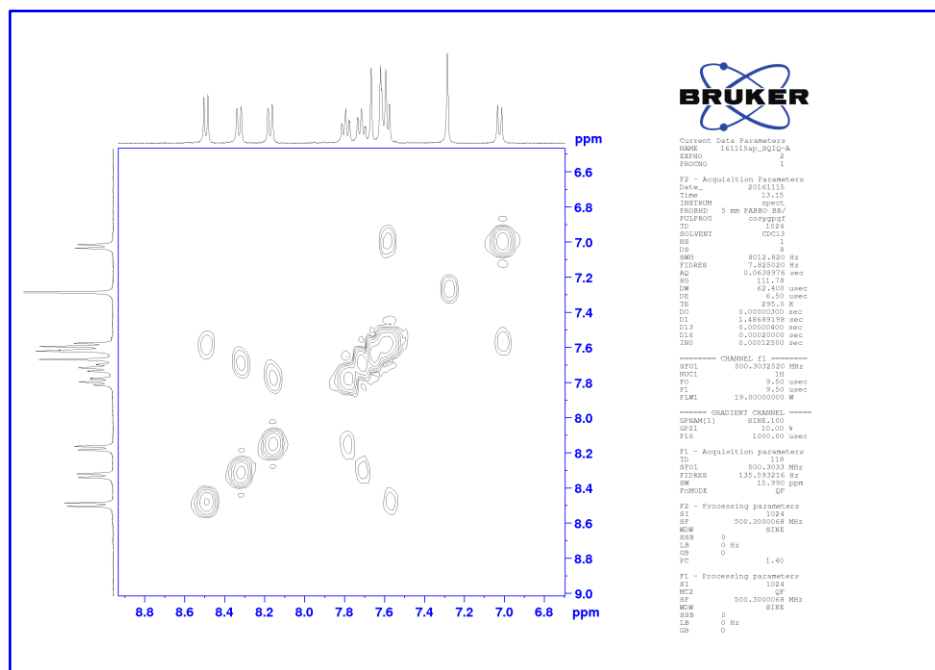


Figure S41. 2D ^1H - ^1H COSY NMR spectrum of **13** in CDCl_3 aromatic region.

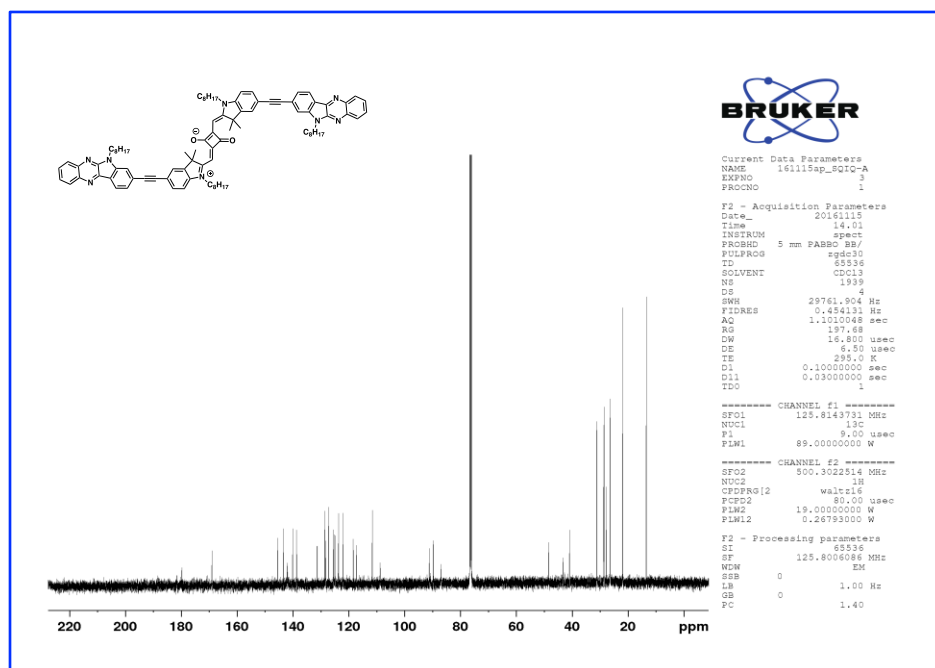


Figure S42. ^{13}C NMR spectra of **13** in CDCl_3

Mass Spectra (MALDI-TOF)

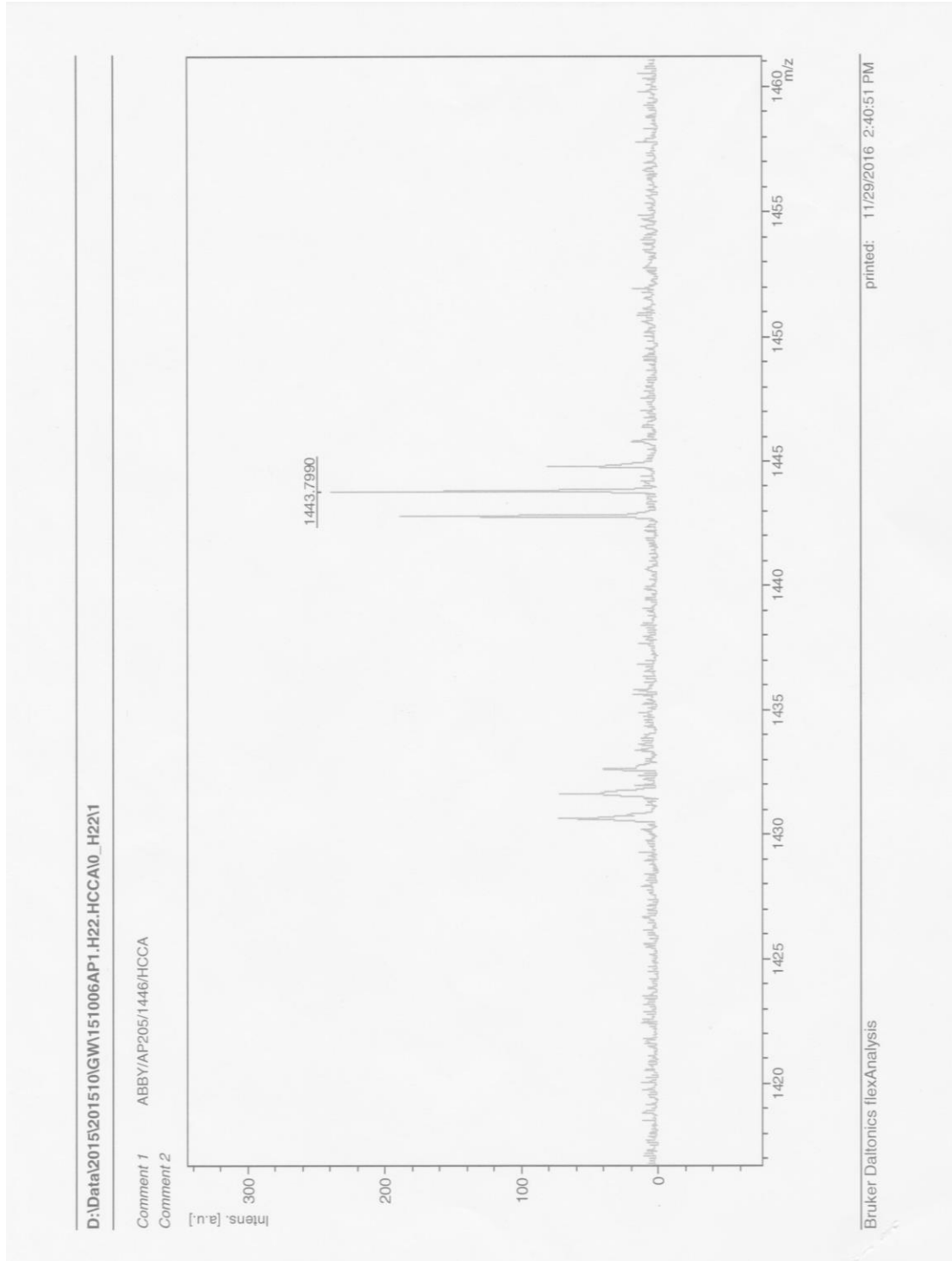


Figure S43. MALDI-TOF mass spectrum of **10**.

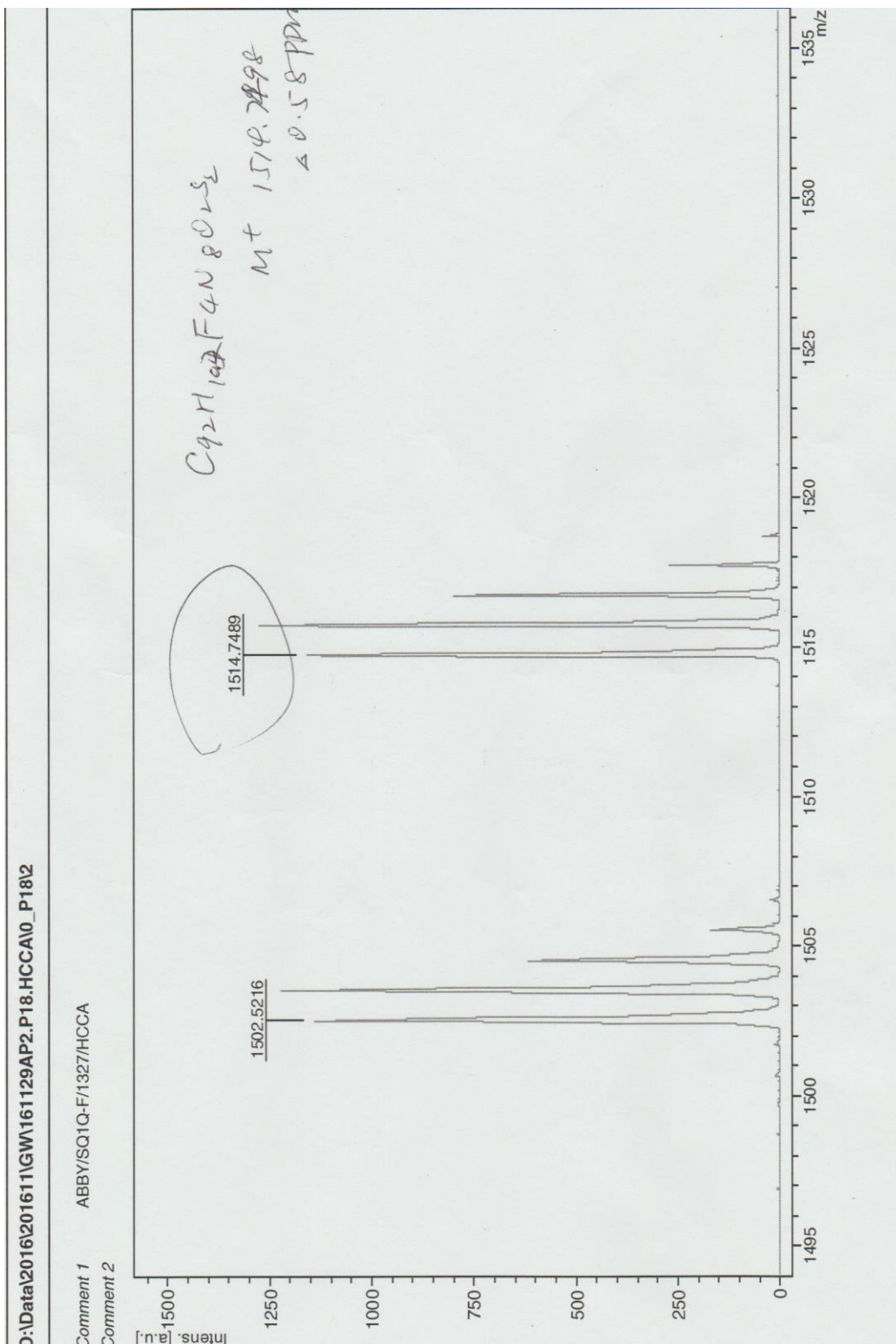
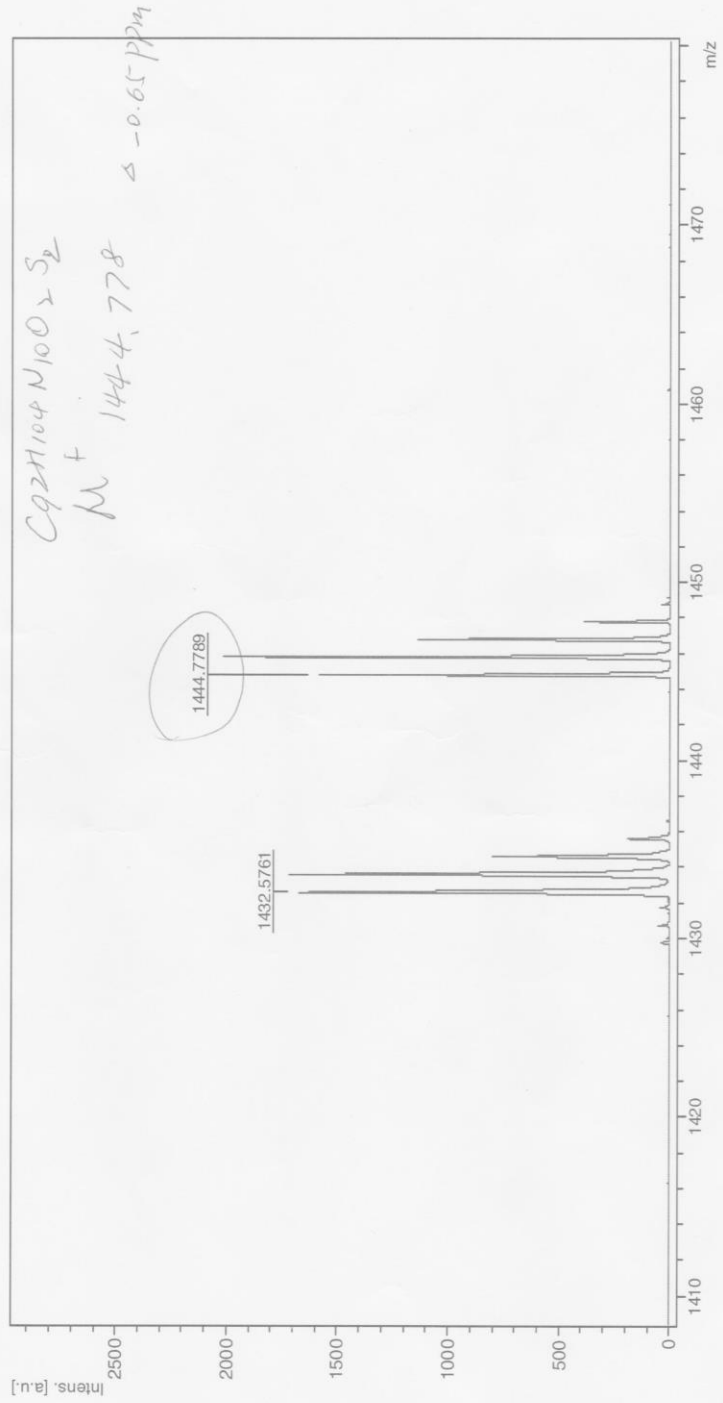


Figure S44. MALDI-TOF mass spectrum of **11**.

D:\Data\2016\201611\GW\161129AP3.B17.HCCA\0_B171

Comment 1 ABBY/SQ1Q-THZ/1444/HCCA

Comment 2



Bruker Daltonics flexAnalysis

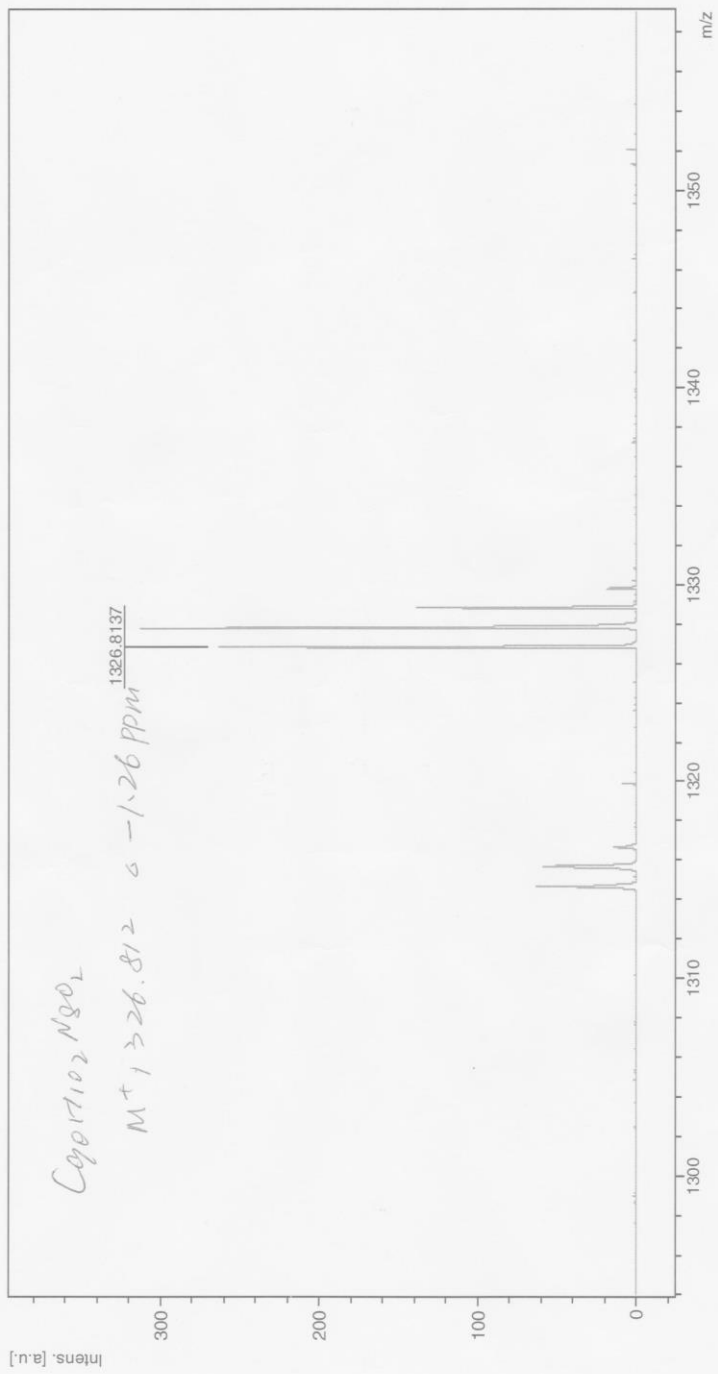
printed: 11/29/2016 3:15:44 PM

Figure S45. MALDI-TOF mass spectrum of **12**.

D:\Data\2016\201611\GW161129AP1.M18.HCCA\0_M18\1

Comment 1 ABBY/SQ1Q-A/1327/HCCA

Comment 2



Bruker Daltonics flexAnalysis

printed: 11/29/2016 2:54:20 PM

Figure S46. MALDI-TOF mass spectrum of **13**.

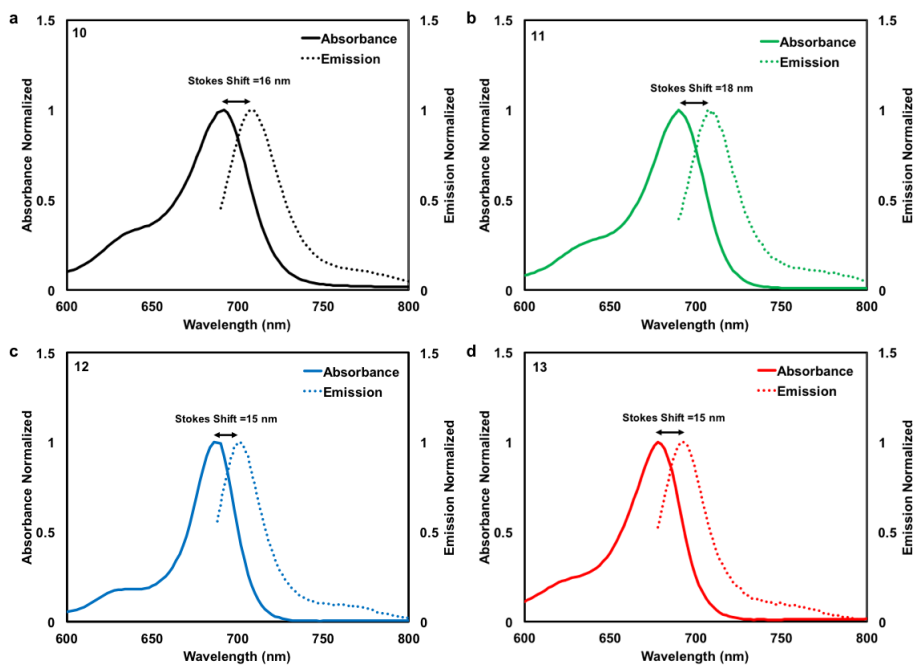


Figure S47. Absorbance and emission spectra of compounds **10-13**.

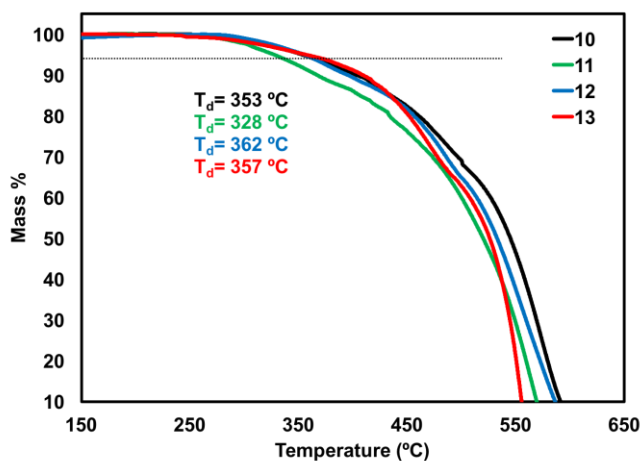


Figure S48. Thermal gravimetric analysis thermogram of **10-13** at a ramp rate of 10 °C/min under a flow of N₂ (100 mL/min).

Computational Details: Gas-phase B3LYP/6-31G(d,p) ground-state equilibrium geometry optimizations were considered within Gaussian 09.⁴ In order to reduce the computational cost while still accounting for the electron-donating ability of the substituent, the solubilizing chains along the conjugated backbone of **10-13** were truncated in all calculations to methyl groups. The dihedral angles that control the relative orientation of the π -systems were systematically altered for these four structures to help ensure that lower energy minima were not missed, where each resulting structure was characterized through frequency calculations at the same level of theory. The low-lying singlet excited states of **10-13** were also calculated using time-dependent density functional theory (TD-DFT) with B3LYP/6-31G(d,p) on the ground-state global minimum geometries. The absorption spectra were simulated through convolution of the vertical transition energies and oscillator strengths with Gaussian functions characterized by a full-width at half-maximum of 3000 cm^{-1} .

Table S1. Calculated vertical transition energies (E, eV), wavelengths (λ , nm), oscillator strengths (f), and dominant electronic configuration for the $S_0 \rightarrow S_{1-15}$ excitations for **10-13** (transitions with less than 0.1 oscillator strength were omitted)

Compound	State	E _{opt} (eV)	λ (nm)	f	Composition
10	S ₁	1.93	641	2.812	H \rightarrow L (92 %)
	S ₃	2.33	533	0.276	H \rightarrow L +2 (91 %)
	S ₆	2.85	435	0.153	H -2 \rightarrow L (90 %)
	S ₁₁	3.16	392	1.057	H -1 \rightarrow L+1 (74 %)
	S ₁₃	3.27	379	0.228	H -4 \rightarrow L +1 (43 %)
11	S ₁	1.96	634	3.059	H \rightarrow L (94 %)
	S ₄	2.39	519	0.158	H \rightarrow L +2 (94 %)
	S ₁₁	3.13	396	0.672	H -1 \rightarrow L +1 (51 %)
	S ₁₃	3.19	389	0.640	H -4 \rightarrow L +1 (34 %)
12	S ₁	2.21	562	1.107	H \rightarrow L (62 %)
	S ₃	2.22	559	1.362	H \rightarrow L +2 (62 %)
	S ₁₃	3.25	382	2.101	H -1 \rightarrow L +1 (36 %)
13	S ₁	1.98	627	3.222	H \rightarrow L (95 %)
	S ₉	3.15	394	0.251	H -1 \rightarrow L +1 (35 %)
	S ₁₁	3.26	381	1.006	H -1 \rightarrow L +1 (48 %)

Density functional results and discussion

DFT and its time dependent-extension (TD-DFT) has proven to be a promising and valuable tool in the rational design of molecules for use in organic electronics.⁵⁻¹⁰ To compare the three π -bridges in addition to the incorporation of fluorine atoms on the terminal indoloquinoxaline unit, DFT was utilized to calculate the predicted geometries, electronic, and optical properties of **10-13**. All DFT calculations were approximated by the B3LYP functional employing the 6-31G(d,p) basis set in Gaussian 09.⁴ The optimized molecular geometries were determined based on the global minima structures (**Figures S49-52**). Changing the π -bridge between the squaraine core and indoloquinoxaline endcap has a marked effect on the overall planarity of the π -conjugated backbone. While the core and endcap are respectively planar as expected, depending on the bridging unit, the dihedral angles between the two is largely affected. For the thiophene bridge, the dihedral angles between the core and endcaps are $< 20^\circ$ resulting in a π -conjugated backbone which is significantly distorted from planarity (**Figures S49 and S50**). This distortion is a result of steric interactions between the H-atoms on the 6 and 5 membered rings adjacent to one another. This distortion is also seen with the thiazole bridging unit, but only between the terminal unit and thiazole. With a N-atom instead of a C-H, there is no longer repulsion between two hydrogens but attraction between the nitrogen lone pair and the adjacent H on the core which allows for planarity between the bridge and the core but not between the bridge and terminal unit (**Figure S51**). On the other hand, the alkyne bridges, as expected, enforce a planar geometry, effectively co-planarizing the squaraine core and indoloquinoxaline end-caps (**Figure S52**).

Regardless of the predicted geometry of these molecules, both the highest occupied molecular orbital (HOMO) and lowest unoccupied molecular orbital (LUMO) are localized on the squaraine core. This indicates that the electronics for this class of materials should be dictated by the squaraine with little to no influence from the indoloquinoxaline terminal unit, which is in-line with the observed optical absorption and electrochemical experiments. However, with the fluorine substituted indoloquinoxaline terminal unit of compound **11**, both the HOMO and LUMO energy levels are stabilized and orbital distributions are predicted to be slightly more delocalized across the π -backbone. Experimentally determined by cyclic voltammetry, the fluorine atoms have less of an effect on the frontier molecular orbitals as predicted by DFT. CV revealed no change in the EA and only a slight increase in IP ($\Delta = 0.04$ eV) upon incorporation of the fluorine atoms. DFT predicted a lowering of the LUMO energy by 0.08 eV and a more drastic lowering of the HOMO energy by 0.17 eV. While the fluorine atoms had minimal effect experimentally, these calculations suggest that a more electron deficient terminal unit may lead to full HOMO/LUMO delocalization of the π -conjugated system and greater influence on the overall electronic properties.

DFT analysis more accurately predicted the influence of the π -bridges on the frontier molecular orbital energy levels where the predicted relative changes in energy levels upon switching from thiophene to thiazole to acetylene correlated with those observed experimentally. The predicted UV-visible absorption spectra for compounds **10-13** were also calculated (**Figures S49-S52**). The calculated vertical transition energies (E, eV), wavelengths (λ , nm), oscillator strengths (f), and dominant electronic configuration for the $S_0 \rightarrow S_{1-15}$ excitations for **10-13** are summarized in **Table S1**. A low energy, high oscillator

strength, HOMO-LUMO transition is predicted because of the bis-indole squaraine core, which correlates with the experimental optical absorption spectra. A second higher energy, low oscillator strength, HOMO-1 to LUMO+1 transition is predicted because of the indoloquinoline terminal unit which also correlates with the experimental optical absorption. Thus, for this system, the high and lower energy portions of the optical absorption can be tailored through modification to indoloquinoline terminal unit and squaraine core, respectively.

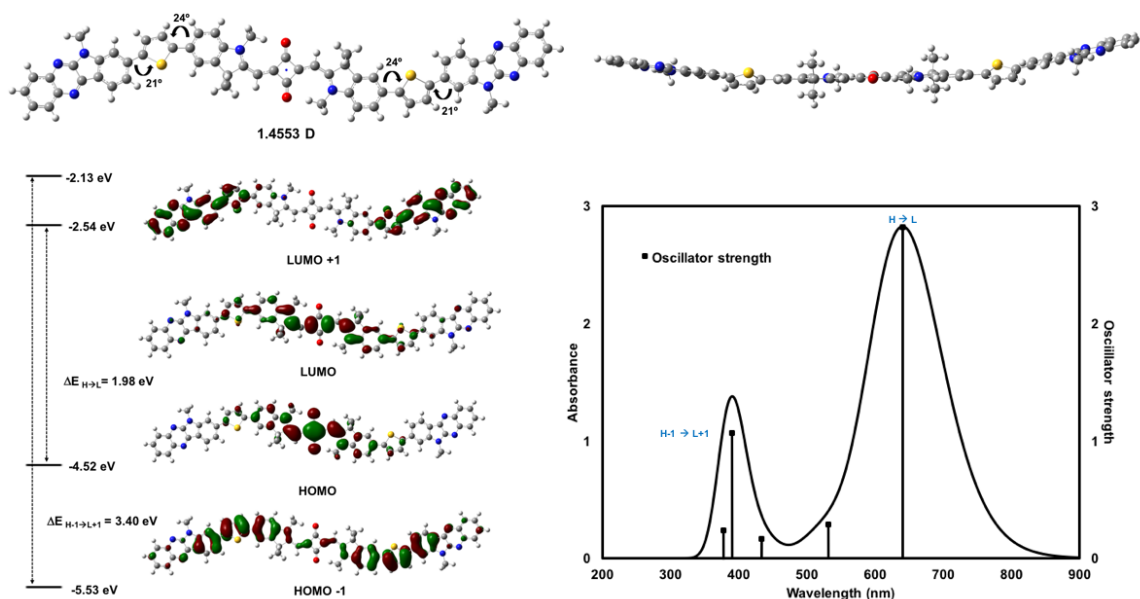


Figure S49. Predicted global minimum ground-state optimized structure of **10** with corresponding dipole moments and dihedral angles. Simulated absorption spectra of **10** and corresponding molecular orbital depiction for the dominate electronic transitions.

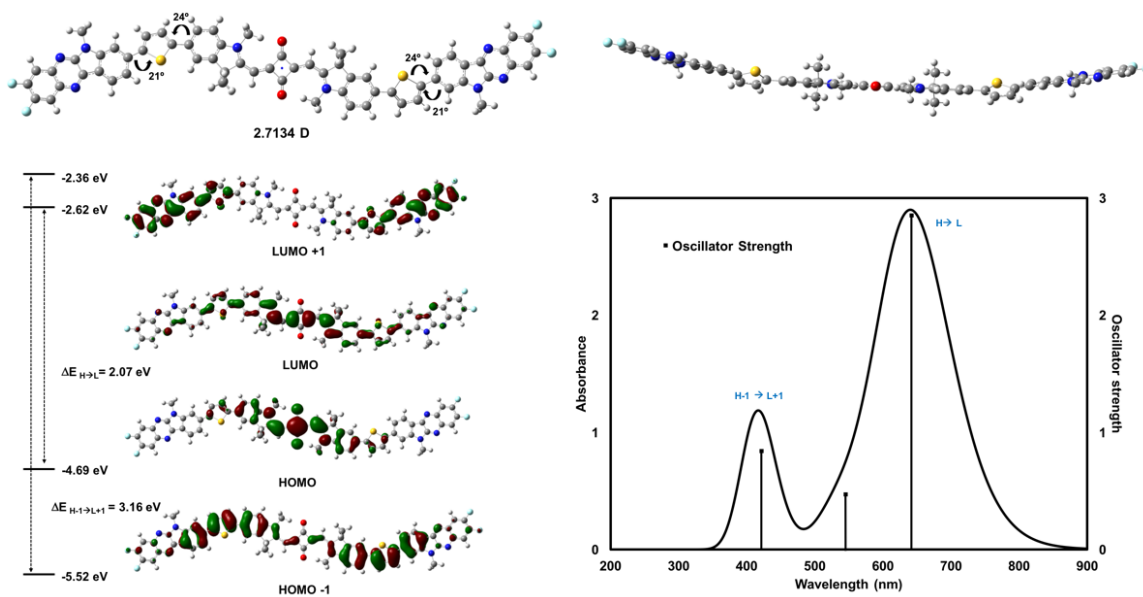


Figure S50. Predicted global minimum ground-state optimized structures of **11** with corresponding dipole moments and dihedral angles. Simulated absorption spectra of **11** and corresponding molecular orbital depiction for the dominate electronic transitions.

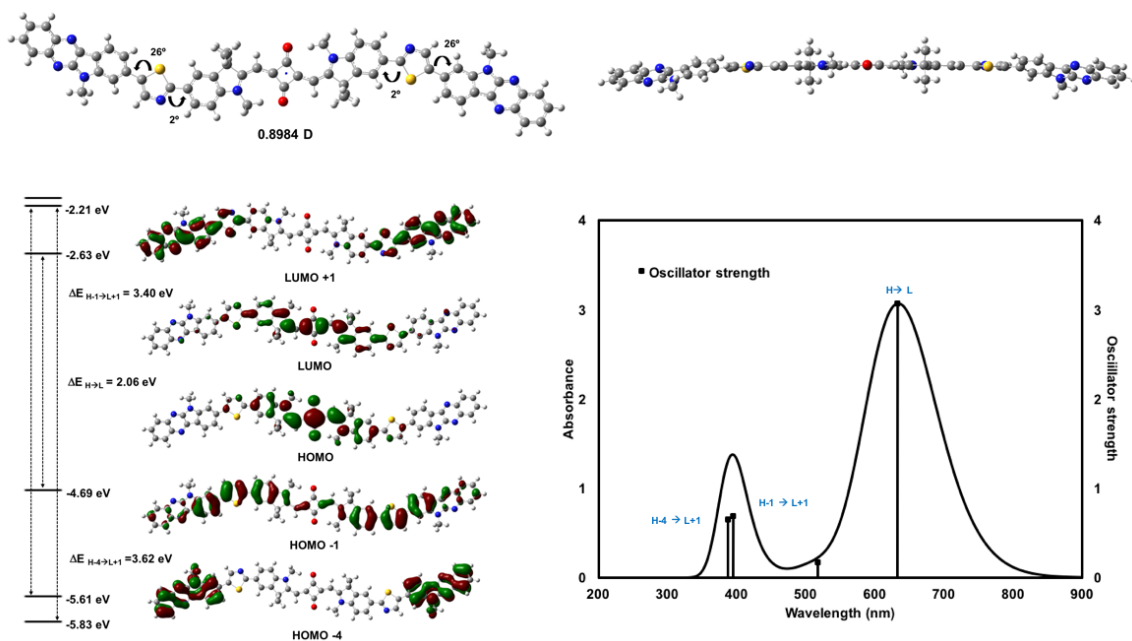


Figure 51. Predicted global minimum ground-state optimized structures of **12** with corresponding dipole moments and dihedral angles. Simulated absorption spectra of **12** and corresponding molecular orbital depiction for the dominate electronic transitions.

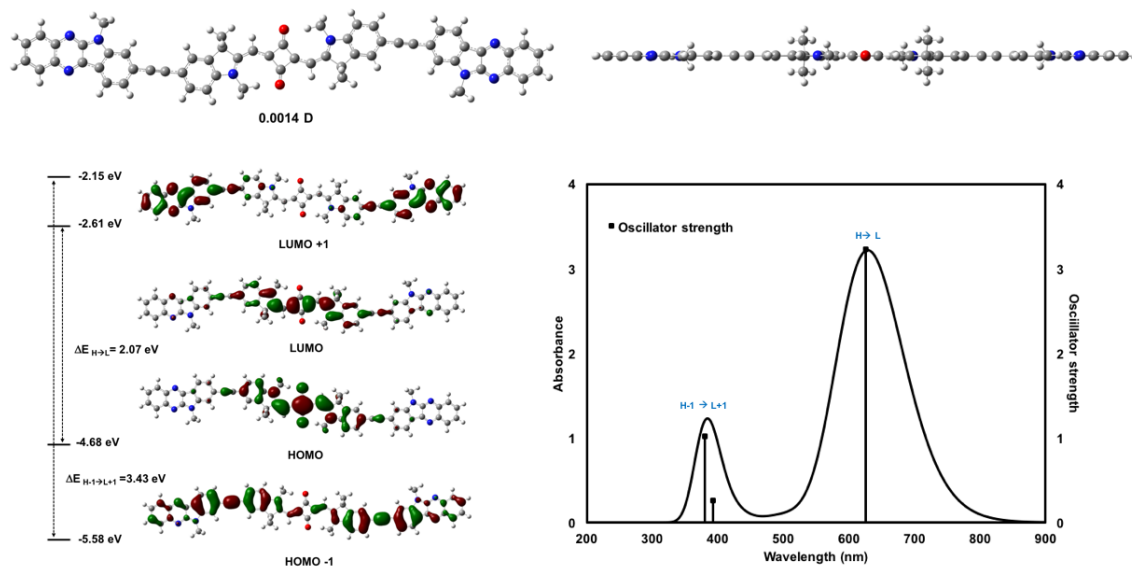


Figure S52. Predicted global minimum ground-state optimized structures of **13** with corresponding dipole moments and dihedral angles. Simulated absorption spectra of **13** and corresponding molecular orbital depiction for the dominate electronic transitions.

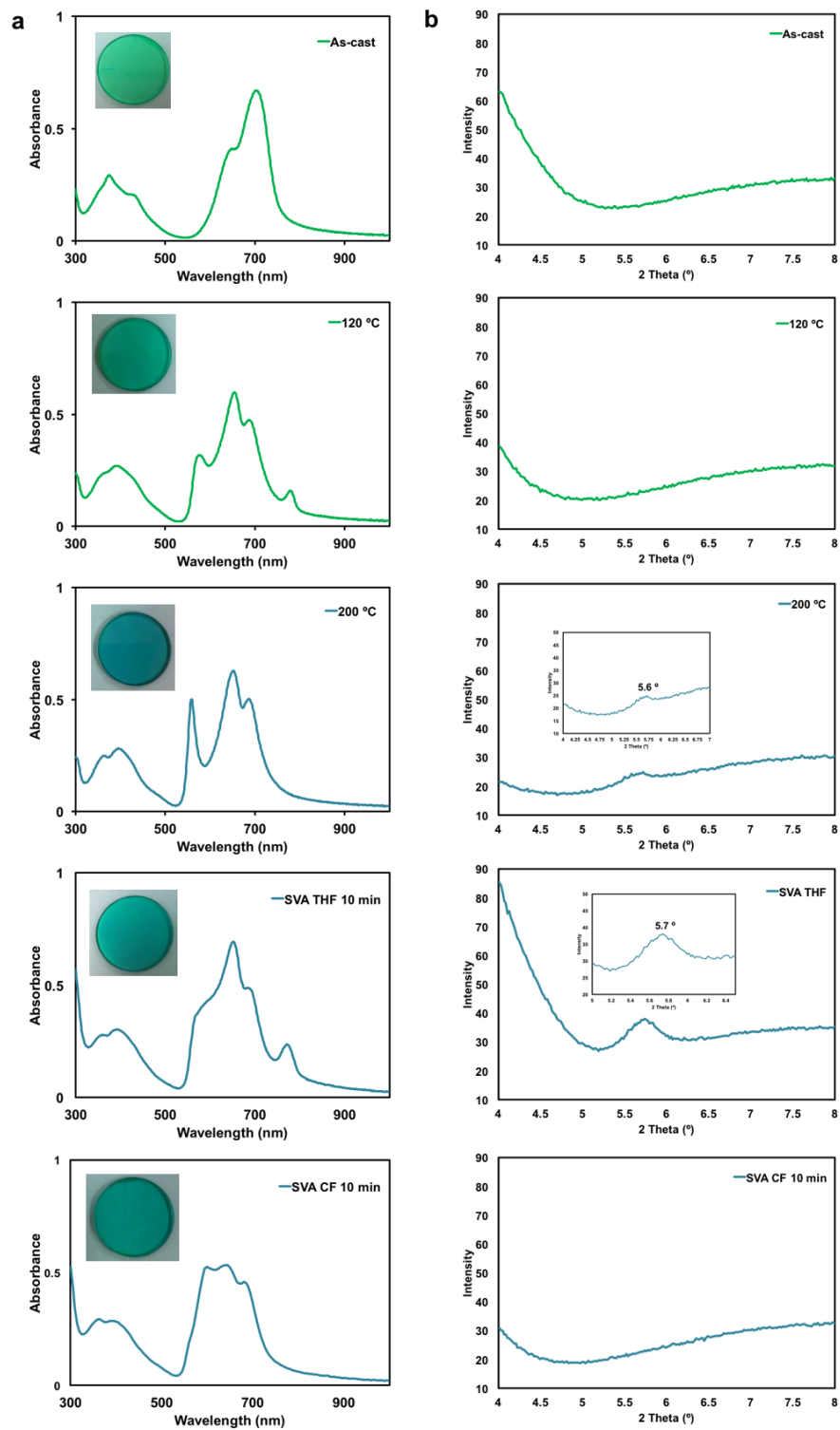


Figure 53. a) UV-Vis and film images of **13** as-cast and after various post deposition treatments. b) Corresponding thin-film XRD patterns.

Table S2. Electrochemical and optical absorption data for squaraine compounds **9b** and **9Th**. Electrochemical properties taken from the solution cyclic voltammetry data. Optical absorption measurements taken in CHCl₃ solution and thin-films on glass spin-cast from CHCl₃ solutions.

	E_{1/2} Oxidation (V)	Oxidation onset (V)	E_{1/2} Reduction (V)	Reduction onset (V)	λ_{max} (nm) solution	λ_{onset} (nm) solution	λ_{max} (nm) film	λ_{onset} (nm) film
9b	0.01, 0.50	-0.16	-1.76	-1.63	590, 639	669	354, 615, 671	721
9Th	-0.09, 0.45	-0.26	-1.86	-1.72	620, 671	705	369, 649, 708	762

References:

- 1 A.-J. Payne, J. S. J. McCahill and G. C. Welch, *Dyes Pigments*, 2015, **123**, 139–146.
- 2 S. Kuster and T. Geiger, *Dyes Pigments*, 2012, **95**, 657–670.
- 3 N. Barbero, C. Magistris, J. Park, D. Saccone, P. Quagliotto, R. Buscaino, C. Medana, C. Barolo and G. Viscardi, *Org. Lett.*, 2015, **17**, 3306–3309.
- 4 M. Frisch, G. Trucks, H. Schlegel, G. Scuseria, M. Robb, J. Cheeseman, G. Scalmani, V. Barone, B. Mennucci, G. Petersson, H. Nakatsuji, M. Caricato, X. Li, H. Hratchian, A. Izmaylov, J. Bloino, G. Zheng, J. Sonnenberg, M. Hada, M. Ehara, K. Toyota, R. Fukuda, J. Hasegawa, M. Ishida, T. Nakajima, Y. Honda, O. Kitao, H. Nakai, T. Vreven, J. Montgomery, J. Peralta, F. Ogliaro, M. Bearpark, J. Heyd, E. Brothers, K. Kudin, V. Staroverov, R. Kobayashi, J. Normand, K. Raghavachari, A. Rendell, J. Burant, S. Iyengar, J. Tomasi, M. Cossi, N. Rega, J. Millam, M. Klene, J. Knox, J. Cross, V. Bakken, C. Adamo, J. Jaramillo, R. Gomperts, R. Stratmann, O. Yazyev, A. Austin, R. Cammi, C. Pomelli, J. Ochterski, R. Martin, K. Morokuma, V. Zakrzewski, G. Voth, P. Salvador, J. Dannenberg, S. Dapprich, A. Daniels, Farkas, J. Foresman, J. Ortiz, J. Cioslowski and D. Fox, *Gaussian 09 Revis. B01 Gaussian Inc Wallingford CT*, 2009.
- 5 Y.-A. Duan, Y. Geng, H.-B. Li, J.-L. Jin, Y. Wu and Z.-M. Su, *J. Comput. Chem.*, 2013, **34**, 1611–1619.
- 6 T. M. McCormick, C. R. Bridges, E. I. Carrera, P. M. DiCarmine, G. L. Gibson, J. Hollinger, L. M. Kozycz and D. S. Seferos, *Macromolecules*, 2013, **46**, 3879–3886.
- 7 M. E. Köse, *J. Phys. Chem. A*, 2012, **116**, 12503–12509.
- 8 L. Pandey, C. Risko, J. E. Norton and J.-L. Brédas, *Macromolecules*, 2012, **45**, 6405–6414.
- 9 L. R. Rutledge, S. M. McAfee and G. C. Welch, *J. Phys. Chem. A*, 2014, **118**, 7939–7951.
- 10 T. Körzdörfer and J.-L. Brédas, *Acc. Chem. Res.*, 2014, **47**, 3284–3291.